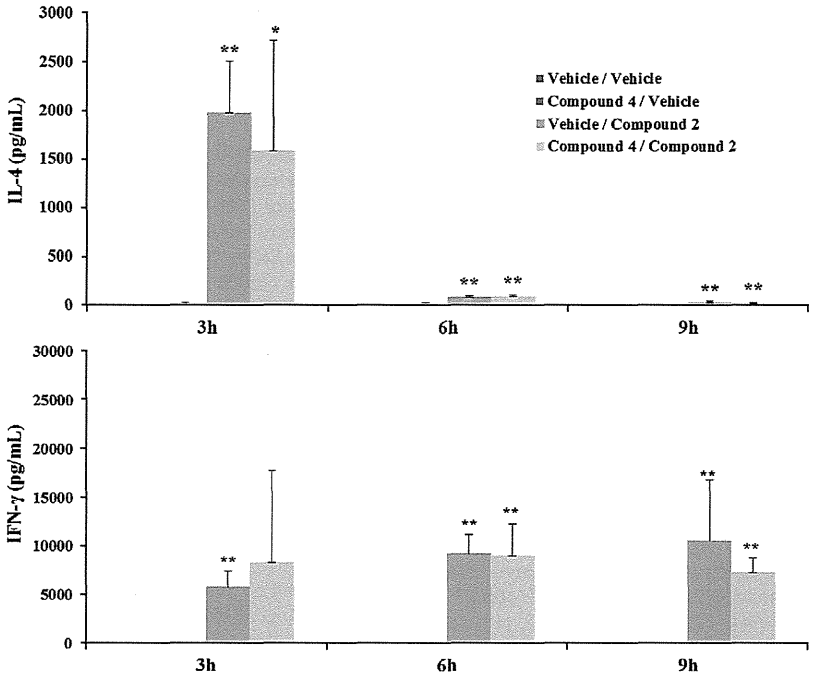

Figure 3. In vivo IL-4/IFN-γ production profile of **2** and **4** after iv administration to C57BL/6 mice. The data are expressed as mean ± SD ($N = 4–5$). $^{**}p < 0.01$, $^{*}p < 0.05$ compared with vehicle group (Student's *t*-test).

the crystal structure of **1**/hCD1d complex[12] was performed utilizing MAESTRO[25] program. Contrary to our expectation, the optimized structure of **2** in the complex had only a subtle, insignificant difference from **1** (Fig. 2). Some of the above derivatives were also calculated in silico, including aromatic derivative **11l** in expectation of aromatic interaction(s), but no significant difference was observed either (data not shown). No significant conformational change in the α1 and α2 helices of CD1d was observed in the minimization initiated from the X-ray structure. Molecular dynamics simulation might be more appropriate for the understanding of this exquisite signaling system.[13]

C-Glycoside derivative (**4**) of **2** was prepared and evaluated for its cytokine inducing profile. Conversion of **1** to its C-glycoside analog **3** is reported to lead to striking enhancement of activity in in vivo animal models of malaria and lung cancer.[8] It is the only example of the C-glycoside which is more potent than corresponding O-glycoside. C-Glycoside (**3**) is shown to somehow stimulate prolonged IL-12 secretion from dendritic cells, followed by prolonged IFN-γ stimulation from NK cells. Compound **4** did not show induction of either cytokines in vitro (Table 2), and in contrast to **3** did not elevate cytokine levels in vivo when administered intravenously to C57BL/6 mice (Fig. 3). In addition, **4** was co-administered intravenously with **2** to evaluate its antagonistic activity. Compound **4** did not antagonize the elevation of IL-4 or IFN-γ levels caused by **2** (Fig. 3). Although the anomeric oxygen does not participate in the hydrogen bond network in the ternary complex with CD1d and NKT T-cell receptor,[11] subtle difference from O to CH_2 was shown to have great influence on the signal transduction.

3. Conclusion

Several analogs related to **1** have been prepared to date, and many of them are equipotent to or even more potent than **1** in the aspect of IFN-γ secretion. In this study, a series of analogs based on **2** with altered ceramide moiety was prepared for its Th2-biased response, and evaluated in the context of IL-4/IFN-γ ratio. Compound **2** in terms of chain length was shown to be one of the optimal compounds for the desired profile. First examples of phytosphingosine-modified analogs were discovered with non-linear hydrocarbon chain or ether linkage that show similar cytokine inducing profile to **2**. Expected aromatic interaction in the sphingosine chain may be of use in the future derivatization. Unprecedented C-glycoside of **2** was prepared and evaluated, which was shown to have no cytokine production effect in vitro or in vivo. In the course of this study, versatile syntheses were developed which allowed preparation of unprecedented derivatives and new findings on Th2 biased immunomodulation. The method and the possibility of structure modification proven in this study should allow future access to the analogs improved in their pharmacological and physicochemical properties.

4. Experimental

4.1. Chemistry

Proton nuclear magnetic resonance spectra (^{1}H NMR) and carbon nuclear magnetic resonance spectra (^{13}C NMR) were recorded on Brucker ARX-400 or Brucker Avance III (400 MHz) spectrometer in the indicated solvent. Chemical shifts (δ) are reported in parts per million relative to the internal standard tetramethylsilane. High-resolution mass spectra (HRMS) and fast atom bombardment (FAB) mass spectra were recorded on JEOL JMS-700 mass spectrometer. Electro-spray ionization (ESI) mass spectra were recorded on Agilent G1956A MSD spectrometer system. Other chemical reagents and solvents were purchased from Aldrich, Tokyo Kasei Kogyo, Wako Pure Chemical Industries, Kanto Kagaku or Nacalai tesque and used without purification. Flash column chromatography was performed using Merck Silica Gel 60 (230–400 mesh) or Purif-Pack® SI 30um supplied by Shoko Scientific. The experimental procedure for alkyl chain derivative **2** is reported

previously.[15] Exemplified procedure for aryl derivative **11l**, alkoxy derivative **11p** and C-glycoside **4**, along with compound data for all compounds **11a–11r** are described.

4.1.1. (2*R*,3*R*,4*R*)-1,3-*O*-Benzylidene-2-*O*-methanesulfonyl-5-phenyl-1,2,3,4-pentanetetrol (6l)

To a suspension of CuI (4.28 g, 22.5 mmol) in THF (45 ml) was added 1.06 M PhLi in THF (85 ml, 90.1 mmol) dropwise at −40 °C and the mixture was stirred for 1 h. A solution of **5** (5.01 g, 22.6 mmol) in THF (15 ml) was added via cannula, and the reaction was slowly allowed to warm to rt over 6 h. The reaction was quenched with satd NH_4Cl aq, extracted with EtOAc and washed twice with half-satd NH_4Cl aq. The organic layer was filtered through Celite, dried over Na_2SO_4 and concentrated. The precipitation formed was filtered and purified by silica gel column chromatography (CH_2Cl_2/MeOH; 3%) to give a colorless solid (6.47 g, 96%). To the solution of this diol (6.40 g, 21.3 mmol) in pyridine (70 ml) was added methanesulfonyl chloride (1.65 ml, 21.3 mmol) at 0 °C, and the mixture was gradually warmed to rt. Pyridine was removed under reduced pressure after consumption of the starting diol, and the residue was diluted with EtOAc, washed twice with water and brine, dried over Na_2SO_4 and concentrated. The residue was purified by silica gel column chromatography (hexane/EtOAc; 50%) to yield **6l** as a colorless solid (2.75 g, 34%). ^{1}H NMR (400 MHz, $CDCl_3$) δ = 7.55–7.52 (m, 2H), 7.44–7.20 (m, 8H), 5.59 (s, 1H), 4.91 (d, J = 1.3 Hz, 1H), 4.52 (dd, J = 1.5, 13.2 Hz, 1H), 4.12 (dd, J = 1.2, 13.3 Hz, 1H), 4.10–4.05 (m, 1H), 3.77 (dd, J = 1.2, 9.0 Hz, 1H), 3.18 (dd, J = 2.8, 13.9 Hz, 1H), 3.13 (s, 3H), 2.78 (dd, J = 7.7, 13.8 Hz, 1H), 2.61 (d, J = 5.2 Hz, 1H).

4.1.2. (2*S*,3*S*,4*R*)-2-Azido-3,4-*O*-isopropylidene-5-phenyl-1,3,4-pentanetriol (7l)

A mixture of **6l** (2.70 g, 7.14 mmol) and NaN_3 (5.57 g, 85.7 mmol) in DMF (35 ml) was stirred at 110 °C for 17 h. The reaction was diluted with EtOAc, washed with water and brine, dried over Na_2SO_4, and concentrated. The residue was purified by silica gel column chromatography (hexane/EtOAc; 40–66%) to yield the azide (892 mg, 38%). To this azide (860 mg, 2.65 mmol) in MeOH (14 ml) was added 6 N HCl (1.3 ml, 7.95 mmol) at 0 °C, and the mixture was stirred for 4 h. The reaction was neutralized with solid K_2CO_3, then filtered, concentrated and purified by silica gel column chromatography (hexane/EtOAc; 40–66%) to yield the triol (434 mg, 69%). The triol (430 mg, 1.81 mmol) was dissolved in 2,2-dimethoxypropane (7 ml), catalytic amount of *p*-toluenesulfonic acid monohydrate (174 mg, 0.092 mmol) was added, and the mixture was stirred for 2 h. MeOH was added and the reaction was stirred for 1 h. The mixture was concentrated and directly purified by silica gel column chromatography (hexane/EtOAc; 17%) to yield **7l** as a colorless oil (350 mg, 70%). ^{1}H NMR (400 MHz, $CDCl_3$) δ = 7.35–7.17 (m, 5H), 4.45 (ddd, J = 3.1, 5.6, 10.2 Hz, 1H), 4.12–4.00 (m, 2H), 3.98–3.88 (m, 1H), 3.65–3.55 (m, 1H), 3.01 (dd, J = 3.0, 14.1 Hz, 1H), 2.81 (dd, J = 10.4, 14.0 Hz, 1H), 2.07 (dd, J = 5.4, 6.8 Hz, 1H), 1.53 (s, 3H), 1.49 (s, 3H).

4.1.3. (2*S*,3*S*,4*R*)-2-Azido-3,4-*O*-isopropylidene-5-phenyl-1-*O*-(2,3,4,6-tetra-*O*-benzyl-α-D-galactosyl)-1,3,4-pentanetriol (9l)

To a mixture of **7l** (175 mg, 0.633 mmol), **8a** (446 mg, 0.822 mmol) and molecular sieves 4 Å in $CHCl_3$ (14 ml) under Ar was added dropwise at −50 °C a solution of $BF_3{\cdot}OEt_2$ (80 μl, 0.631 mmol) in $CHCl_3$ (2.7 ml). After 1 h of stirring the reaction was quenched with satd $NaHCO_3$ aq, extracted with CH_2Cl_2, washed with brine, dried over Na_2SO_4, concentrated and purified by silica gel column chromatography (hexane/EtOAc; 12.5%) to give **9l** as a colorless oil (108 mg, 21%). ^{1}H NMR (400 MHz, $CDCl_3$) δ = 7.40–7.15 (m, 25H), 4.96 (d, J = 3.7 Hz, 1H), 4.95 (d, J = 11.2 Hz, 1H), 4.84 (d, J = 12.2 Hz, 1H), 4.81 (d, J = 13.0 Hz, 1H), 4.72 (d, J = 11.8 Hz, 1H), 4.71 (d, J = 12.0 Hz, 1H), 4.57 (d, J = 11.5 Hz, 1H), 4.48 (d, J = 11.9 Hz, 1H), 4.41 (d, J = 12.1 Hz, 1H), 4.42–4.33 (m, 1H), 4.20–3.90 (m, 6H), 3.77 (dd, J = 6.5, 10.8 Hz, 1H), 3.65–3.45 (m, 3H), 3.00 (dd, J = 2.8, 14.1 Hz, 1H), 2.78 (dd, J = 10.5, 14.0 Hz, 1H), 1.44 (s, 3H), 1.23 (s, 3H).

4.1.4. (2*S*,3*S*,4*R*)-3,4-*O*-Isopropylidene-5-phenyl-1-*O*-(2,3,4,6-tetra-*O*-benzyl-α-D-galactosyl)-2-tetracosanoylamino-1,3,4-pentanetriol (10l)

A mixture of **9l** (98.2 mg, 0.123 mmol) and Lindlar catalyst (98 mg) in EtOH (5 ml) was stirred under H_2 atmosphere for 24 h. Additional Lindlar catalyst (96 mg) was added and the mixture was stirred for another 24 h. Insolubles were removed by filtration through membrane filter and the filtrate was concentrated to give an oil. The oil was diluted with CH_2Cl_2 (2 ml) and 1-ethyl-3-(3-dimethylaminopropyl) carbodiimide hydrochloride (26.8 mg, 0.140 mmol) was added. This mixture was added at 0 °C to the premixed suspension of Lignoceric acid (44.8 mg, 0.122 mmol), 1-hydroxybenzotrilazole (20.3 mg, 0.150 mmol) and Hunig's Base (49 μl, 0.281 mmol), in DMF (2.5 ml) and CH_2Cl_2 (5 ml), and the mixture was stirred at rt for 24 h. The reaction mixture was diluted with [Et_2O/EtOAc = 1:1] solution, quenched with satd $NaHCO_3$ aq, washed with 1 N HCl and brine, dried over Na_2SO_4, concentrated and purified by silica gel column chromatography (hexane/EtOAc; 25–33%) to give **10l** as a colorless solid (90.0 mg, 65% in two steps). ^{1}H NMR (400 MHz, $CDCl_3$) δ = 7.40–7.08 (m, 25H), 6.32 (d, J = 8.4 Hz, 1H), 4.924 (d, J = 11.4 Hz, 1H), 4.919 (d, J = 3.9 Hz, 1H), 4.82 (d, J = 11.4 Hz, 1H), 4.81 (d, J = 11.7 Hz, 1H), 4.74 (d, J = 11.7 Hz, 1H), 4.66 (d, J = 11.5 Hz, 1H), 4.58 (d, J = 11.6 Hz, 1H), 4.47 (d, J = 11.8 Hz, 1H), 4.37 (d, J = 11.8 Hz, 1H), 4.25–4.05 (m, 4H), 4.06 (dd, J = 3.3, 9.7 Hz, 1H), 3.98 (t, J = 6.1 Hz, 1H), 3.95–3.90 (m, 2H), 3.65 (d, J = 11.2 Hz, 1H), 3.55 (dd, J = 7.0, 9.5 Hz, 1H), 3.38 (dd, J = 5.6, 9.4 Hz, 1H), 2.75–2.70 (m, 2H), 2.18–1.93 (m, 2H), 1.60–1.50 (m, 2H), 1.47 (s, 3H), 1.28 (s, 3H), 1.35–1.20 (m, 40H), 0.87 (t, J = 6.5 Hz, 3H).

4.1.5. (2*S*,3*S*,4*R*)-1-*O*-(α-D-Galactosyl)-5-phenyl-2-tetracosanoylamino-1,3,4-pentanetriol (11l)

To a solution of **10l** (90.0 mg, 0.0801 mmol) in CH_2Cl_2 (5 ml) and MeOH (1 ml) was added 4 M HCl in dioxane (100 μl, 0.4 mmol) at 0 °C and the mixture was stirred at rt for 3 h. Silica gel was added to the reaction mixture, then volatiles were removed under reduced pressure. The residue was purified by silica gel column chromatography (hexane/EtOAc; 25–33%) to give a colorless solid (68 mg, 78%). A mixture of this solid (67 mg, 0.062 mmol) and Pearlman's catalyst (26.8 mg) in $CHCl_3$ (1 ml) and MeOH (3 ml) was stirred under H_2 atmosphere for 1.5 h. Insolubles were removed by filtration through membrane filter and the filtrate was concentrated to give compound **11l** as a colorless solid (43.6 mg, 98%). ^{1}H NMR (400 MHz, Pyr-d_5) δ = 8.53 (d, J = 8.8 Hz, 1H), 7.62 (d, J = 6.8 Hz, 2H), 7.32–7.27 (m, 2H), 7.20–7.17 (m, 1H), 6.83 (d, J = 4.6 Hz, 1H), 6.58–6.44 (m, 3H), 6.33 (d, J = 6.7 Hz, 1H), 6.27 (d, J = 4.0 Hz, 1H), 5.51 (d, J = 3.9 Hz, 1H), 5.27 (qd, J = 4.7, 8.9 Hz, 1H), 4.69–4.59 (m, 2H), 4.58–4.31 (m, 8H), 3.70 (dd, J = 1.8, 13.5 Hz, 1H), 3.14 (dd, J = 9.3, 13.7 Hz, 1H), 2.49–2.38 (m, 2H), 1.81 (quin, J = 7.5 Hz, 2H), 1.39–1.18 (m, 40H), 0.87 (t, J = 6.7 Hz, 3H); ^{13}C NMR (101 MHz, Pyr-d_5) δ = 173.4, 130.5, 128.5, 101.8, 76.6, 74.0, 73.1, 71.6, 71.0, 70.4, 69.3, 62.7, 51.7, 40.7, 36.8, 32.1, 30.0, 30.0, 29.9, 29.9, 29.8, 29.6, 26.4, 23.0, 14.3; HRMS (FAB) Calcd for $C_{41}H_{73}NNaO_9^+$: 746.5178; Found: 746.5157.

4.1.6. (2*R*,3*R*,4*R*)-1,3-*O*-Benzylidene-2-*O*-methanesulfonyl-6-oxa-1,2,3,4-nonanetetrol (6p)

NaH (1.82 g, 45.4 mmol) was added to 1-propanol (60 ml) at 0 °C and stirred for 5 min. To the solution was added **5** (2.00 g, 9.01 mmol), and the mixture was stirred at rt for 20 h. To the reac-

tion mixture was added water (200 mL), and the product was extracted with EtOAc (200 mL × 1, 50 ml × 2). The combined organic layer was dried over Na_2SO_4, filtered, concentrated and purified over silica gel column chromatography (hexane/EtOAc; 50–67%) to yield the ether as a colorless solid (2.12 g, 83%). To the solution of above ether (451 mg, 1.60 mmol) in pyridine (15 ml) was added methanesulfonyl chloride (118 μl, 1.51 mmol) at −40 °C, and the mixture was gradually warmed to rt. After 36 h of stirring pyridine was removed azeotropically with heptane. The residue was directly purified by column chromatography (hexane/EtOAc; 40–66%) to yield **6p** as a colorless solid (357.0 mg, 62%). ^{1}H NMR (400 MHz, $CDCl_3$) δ = 7.52–7.44 (m, 2H), 7.41–7.35 (m, 3H), 5.58 (s, 1H), 4.88 (dd, J = 1.5, 3.0 Hz, 1H), 4.59 (dd, J = 1.6, 13.2 Hz, 1H), 4.16 (dd, J = 1.3, 13.2 Hz, 1H), 4.04 (dd, J = 1.5, 9.2 Hz, 1H), 4.00–3.93 (m, 1H), 3.67 (dd, J = 2.9, 9.8 Hz, 1H), 3.63 (dd, J = 4.4, 9.8 Hz, 1H), 3.47 (ddd, J = 6.7, 9.5, 13.8 Hz, 2H), 3.17 (s, 3H), 2.76 (d, J = 6.4 Hz, 1H), 1.61 (sxt, J = 7.1 Hz, 2H), 0.93 (t, J = 7.5 Hz, 3H); MS (ESI) 361.1 $(M+H)^+$.

4.1.7. (2*S*,3*S*,4*R*)-2-Azido-3,4-*O*-isopropylidene-6-oxa-1,3,4-nonanetriol (7p)

A mixture of **6p** (325 mg, 0.901 mmol) and Pearlman's catalyst (61.3 mg, 0.437 mmol) in EtOH (10 ml) was stirred under H_2 atmosphere at rt for 90 min. Insolubles were removed by filtration through membrane filter and the filtrate was concentrated to give a colorless oil which contained EtOH (281.3 mg, calculated from ^{1}H NMR to contain 242 mg of the triol, 99%). EtOAc was added and removed under reduced pressure repeatedly for three times to remove EtOH. The residue was dissolved in DMF (5 ml), NaN_3 (236 mg, 3.63 mmol) was added and the mixture was stirred under Ar at 95 °C for 3 h. To the reaction mixture was added half-satd $NaHCO_3$ (100 mL), and the product was extracted with EtOAc (100 mL × 1, 50 ml × 8). The combined organic layer was dried over Na_2SO_4, filtered, concentrated and purified by silica gel column chromatography ([hexane/EtOAc = 1:1]/MeOH; 2–5%) to give the azido-triol as a colorless oil (119.0 mg, 60%). The residue was dissolved in 2,2-dimethoxypropane (2 ml), catalytic amount of *p*-toluenesulfonic acid monohydrate (5 mg, 0.026 mmol) was added at 0 °C, and the mixture was stirred for 21 h during which ice in the cooling bath gradually melted. MeOH was added and the reaction was stirred for 2 h. To the mixture was added half-satd $NaHCO_3$ aq (75 mL), and the product was extracted with EtOAc (75 mL × 1, 40 ml × 2). The combined organic layer was dried over Na_2SO_4, filtered, concentrated and purified by silica gel column chromatography (hexane/EtOAc; 20–50%, then to [hexane/EtOAc = 1:1]/MeOH; 5%) to yield **7p** as a colorless oil (36.9 mg, 26%). ^{1}H NMR (400 MHz, DMSO-d_6) δ = 5.10 (br s, 1H), 4.23 (q, J = 5.8 Hz, 1H), 3.93 (dd, J = 5.9, 9.0 Hz, 1H), 3.80 (dd, J = 1.5, 11.0 Hz, 1H), 3.62 (dd, J = 5.0, 10.5 Hz, 1H), 3.60–3.49 (m, 2H), 3.46 (dd, J = 5.8, 10.5 Hz, 1H), 3.39 (t, J = 6.7 Hz, 2H), 1.53 (sxt, J = 7.1 Hz, 2H), 1.34 (s, 3H), 1.25 (s, 3H), 0.87 (t, J = 7.4 Hz, 3H); ^{13}C NMR (101 MHz, DMSO-d_6) δ = 107.8, 75.6, 74.5, 72.3, 68.7, 62.2, 61.6, 27.4, 25.2, 22.2, 10.4; MS (ESI) 232.2 $(M-N_2+H)^+$.

4.1.8. (2*S*,3*S*,4*R*)-2-Azido-3,4-*O*-isopropylidene-6-oxa-1-*O*-(2,3,4,6-tetra-*O*-benzyl-α-D-galactosyl)-1,3,4-nonanetriol (9p)

To a solution of **7p** (36.9 mg, 0.142 mmol) in toluene (3 ml) under Ar were added molecular sieves 4 Å (151.3 mg), a solution of tetra-*O*-benzyl-galactosyl chloride **8b** (162 mg, 0.29 mmol) in toluene (7 ml), tetra-*n*-butylammonium bromide (140.9 mg, 0.437 mmol) and Hunig's Base (50 μl, 0.286 mmol) at rt. The mixture was stirred at rt for 45 min, at 60 °C for 45 h, and at 80 °C for 15 h. MeOH was added at 50 °C and stirred for 6 h. The reaction mixture was passed through Celite pad to remove insolubles, and to the filtrate was added half-satd $NaHCO_3$ aq (100 ml). The product was extracted with EtOAc (100 ml × 1, 50 ml × 1), and the combined organic layer was dried over Na_2SO_4, filtered, concentrated and subjected to silica gel column chromatography (hexane/EtOAc; 11% to 14%) to give **9p** as a colorless oil (98.0 mg) as a mixture with tetra-*O*-benzyl-1-methoxygalactose. Tetra-*O*-benzyl-1-methoxygalactose was removed in the next step. MS (FAB) 804 $(M+Na)^+$.

4.1.9. (2*S*,3*S*,4*R*)-3,4-*O*-Isopropylidene-6-oxa-1-*O*-(2,3,4,6-tetra-*O*-benzyl-α-D-galactosyl)-2-tetracosanoylamino-1,3,4-nonanetriol (10p)

The crude **9p** obtained in 4.1.8 was divided into two portions. One portion was dissolved in EtOH (3 ml) and stirred with Lindlar catalyst (20.8 mg) under H_2 atmosphere for 22 h. Insolubles were removed by filtration through membrane filter and the filtrate was concentrated to give an oil. The oil was diluted with CH_2Cl_2 (1 ml) and DMF (1 ml), and to the solution was added premixed suspension of Lignoceric acid (10.5 mg, 0.028 mmol), 3*H*-[1,2,3]-triazolo[4,5-*b*]pyridin-3-ol (4.5 mg, 0.033 mmol) and 1-ethyl-3-(3-dimethylaminopropyl) carbodiimide hydrochloride (7.4 mg, 0.039 mmol) in DMF (1 ml) and CH_2Cl_2 (1 ml), then Hunig's Base (12 μl, 0.069 mmol), and the mixture was stirred at 35 °C for 17 h. To the reaction mixture was added half-satd $NaHCO_3$ aq (100 mL), and the product was extracted with [hexane/EtOAc = 1:1] solution (100 mL × 1, 50 ml × 2). The combined organic layer was dried over Na_2SO_4, filtered, concentrated and purified by silica gel column chromatography (hexane/EtOAc; 25%) to give **10p** as colorless oil (17.8 mg). The same procedure was applied to the other portion of the crude **9p**, and the products from both portions were combined to yield 35.1 mg (22% from **7p**) as a colorless oil. ^{1}H NMR (400 MHz, $CDCl_3$) δ = 7.42–7.19 (m, 20H), 6.36 (d, J = 9.4 Hz, 1H), 4.93 (d, J = 11.5 Hz, 1H), 4.89 (d, J = 3.8 Hz, 1H), 4.81 (d, J = 11.4 Hz, 1H), 4.80 (d, J = 11.4 Hz, 1H), 4.74 (d, J = 11.7 Hz, 1H), 4.66 (d, J = 11.5 Hz, 1H), 4.58 (d, J = 11.5 Hz, 1H), 4.48 (d, J = 11.8 Hz, 1H), 4.38 (d, J = 11.9 Hz, 1H), 4.23–4.02 (m, 5H), 3.98–3.88 (m, 3H), 3.61 (dd, J = 2.6, 11.4 Hz, 1H), 3.54 (dd, J = 6.8, 9.3 Hz, 1H), 3.45–3.34 (m, 4H), 3.30 (td, J = 7.0, 9.4 Hz, 1H), 2.10–1.94 (m, 2H), 1.61–1.52 (m, 4H), 1.44 (s, 3H), 1.33 (s, 3H), 1.32–1.19 (m, 40H), 0.88 (t, J = 7.2 Hz, 3H), 0.87 (t, J = 7.3 Hz, 3H); ^{13}C NMR (101 MHz, $CDCl_3$) δ = 138.3, 128.5, 128.4, 128.4, 128.3, 128.3, 128.0, 127.9, 127.7, 127.6, 127.5, 108.7, 99.6, 78.9, 74.7, 74.6, 73.5, 73.4, 73.0, 36.8, 31.9, 29.7, 29.7, 29.6, 29.4, 29.4, 25.8, 25.6, 22.7, 14.1, 10.4; MS (FAB) 1128 $(M+Na-1)^+$.

4.1.10. (2*S*,3*S*,4*R*)-1-*O*-(α-D-Galactosyl)-6-oxa-2-tetracosanoylamino-1,3,4-nonanetriol (11p)

To a solution of **10p** (16.4 mg, 0.015 mmol) in CH_2Cl_2 (4 ml) and MeOH (0.8 ml) was added 4 M HCl in dioxane (80 μl, 0.320 mmol) and the mixture was stirred at rt for 2 h. Et_3N (90 μl, 0.646 mmol) was added, then volatiles were removed under reduced pressure to give solid, which was purified by silica gel column chromatography (hexane/EtOAc; 33% to 44%) to give colorless solid (13.8 mg, 87%). A mixture of above solid (12.5 mg, 0.012 mmol) and Pearlman's catalyst (7.5 mg) in CH_2Cl_2 (1 ml) and MeOH (3 ml) was stirred under H_2 atmosphere for 3.5 h. Insolubles were removed by filtration through membrane filter and the filtrate was concentrated to give compound **11p** as a colorless solid (8.8 mg, quant.) ^{1}H NMR (400 MHz, Pyr-d_5) δ = 8.45 (d, J = 8.7 Hz, 1H), 6.86 (d, J = 6.7 Hz, 1H), 6.53 (d, J = 6.1 Hz, 1H), 6.50–6.41 (m, 2H), 6.34 (d, J = 6.4 Hz, 1H), 6.27 (d, J = 4.1 Hz, 1H), 5.54 (d, J = 3.8 Hz, 1H), 5.30–5.21 (m, 1H), 4.69–4.59 (m, 2H), 4.57–4.53 (m, 1H), 4.53–4.34 (m, 7H), 4.12 (dd, J = 2.7, 9.9 Hz, 1H), 3.99 (dd, J = 6.0, 9.9 Hz, 1H), 3.45 (tq, J = 6.7, 9.1 Hz, 2H), 2.42 (dt, J = 1.8, 7.5 Hz, 2H), 1.79 (quin, J = 7.5 Hz, 2H), 1.54 (sxt, J = 7.1 Hz, 2H), 1.39–1.15 (m, 40H), 0.87 (t, J = 6.8 Hz, 3H), 0.82 (t, J = 7.5 Hz, 3H); ^{13}C NMR (101 MHz, Pyr-d_5) δ = 173.4, 101.6, 74.2, 74.1, 73.3, 73.1, 72.1, 71.7, 71.0, 70.4, 68.7, 62.7, 51.6, 36.8, 32.1, 30.0, 30.0, 29.9, 29.9, 29.8, 29.8, 29.6,

26.4, 23.3, 23.0, 14.3, 10.8; HRMS (FAB) Calcd for $C_{38}H_{75}NNaO_{10}^+$: 728.5283; Found: 728.5311.

4.1.11. (2*S*,3*S*,4*R*)-1-*O*-(α-D-Galactosyl)-2-tetracosanoylamino-1,3,4-heptanetriol (11a)

^{1}H NMR (400 MHz, Pyr-d_5) δ = 8.40 (d, J = 8.5 Hz, 1H), 6.91 (d, J = 6.1 Hz, 1H), 6.59 (d, J = 6.1 Hz, 1H), 6.48 (t, J = 5.6 Hz, 1H), 6.38 (d, J = 6.1 Hz, 1H), 6.26 (d, J = 3.9 Hz, 1H), 6.03 (d, J = 5.9 Hz, 1H), 5.57 (d, J = 3.8 Hz, 1H), 5.30–5.21 (m, 1H), 4.70–4.61 (m, 2H), 4.58–4.53 (m, 1H), 4.53–4.47 (m, 1H), 4.47–4.34 (m, 4H), 4.33–4.23 (m, 2H), 2.43 (t, J = 7.5 Hz, 2H), 2.27–2.14 (m, 1H), 1.94–1.75 (m, 4H), 1.74–1.57 (m, 1H), 1.41–1.14 (m, 40H), 0.96 (t, J = 7.3 Hz, 3H), 0.87 (t, J = 6.9 Hz, 3H); ^{13}C NMR (101 MHz, Pyr-d_5) δ = 173.2, 101.6, 76.9, 73.1, 72.2, 71.7, 71.0, 70.3, 68.7, 62.7, 51.4, 36.8, 36.6, 32.1, 30.0, 30.0, 29.9, 29.9, 29.8, 29.8, 29.6, 26.4, 23.0, 19.6, 14.6, 14.3; HRMS (FAB) Calcd for $C_{37}H_{73}NNaO_9^+$: 698.5178; Found: 698.5151.

4.1.12. (2*S*,3*S*,4*R*)-1-*O*-(α-D-Galactosyl)-2-tricosanoylamino-1,3,4-octanetriol (11b)

^{1}H NMR (400 MHz, Pyr-d_5) δ = 8.42 (d, J = 8.7 Hz, 1H), 5.57 (d, J = 3.8 Hz, 1H), 5.31–5.21 (m, 1H), 4.70–4.62 (m, 2H), 4.58–4.54 (m, 1H), 4.54–4.48 (m, 1H), 4.46–4.35 (m, 4H), 4.32–4.24 (m, 2H), 2.44 (t, J = 7.2 Hz, 2H), 2.32–2.17 (m, 1H), 1.90–1.74 (m, 4H), 1.70–1.53 (m, 1H), 1.46–1.16 (m, 40H), 0.91–0.80 (m, 6H); ^{13}C NMR (101 MHz, Pyr-d_5) δ = 173.3, 101.6, 76.8, 73.1, 72.5, 71.6, 71.1, 70.3, 68.7, 62.7, 51.4, 36.8, 34.1, 32.1, 30.0, 29.9, 29.9, 29.8, 29.8, 29.6, 28.6, 26.4, 23.3, 23.0, 14.4, 14.3; HRMS (FAB) Calcd for $C_{37}H_{73}NNaO_9^+$: 698.5178; Found: 698.5161.

4.1.13. (2*S*,3*S*,4*R*)-1-*O*-(α-D-Galactosyl)-2-tetracosanoylamino-1,3,4-octanetriol (11c)

^{1}H NMR (400 MHz, Pyr-d_5) δ = 8.41 (d, J = 8.7 Hz, 1H), 6.96–6.86 (m, 1H), 6.65–6.53 (m, 1H), 6.53–6.43 (m, 1H), 6.37 (d, J = 6.1 Hz, 1H), 6.31–6.20 (m, 1H), 6.03 (d, J = 5.1 Hz, 1H), 5.57 (d, J = 3.9 Hz, 1H), 5.31–5.21 (m, 1H), 4.71–4.62 (m, 2H), 4.55 (br s, 1H), 4.53–4.48 (m, 1H), 4.47–4.35 (m, 4H), 4.32–4.22 (m, 2H), 2.43 (t, J = 7.2 Hz, 2H), 2.32–2.18 (m, 1H), 1.91–1.72 (m, 4H), 1.67–1.53 (m, 1H), 1.47–1.15 (m, 42H), 0.87 (t, J = 6.8 Hz, 3 H), 0.85 (t, J = 6.9 Hz, 3H); ^{13}C NMR (101 MHz, Pyr-d_5) δ = 173.2, 101.6, 76.9, 73.1, 72.5, 71.7, 71.1, 70.3, 68.7, 62.7, 51.4, 36.8, 34.1, 32.1, 30.0, 30.0, 29.9, 29.9, 29.8, 29.8, 29.6, 28.6, 26.4, 23.3, 23.0, 14.4, 14.3; HRMS (FAB) Calcd for $C_{38}H_{75}NNaO_9^+$: 712.5334; Found: 712.5316.

4.1.14. (2*S*,3*S*,4*R*)-1-*O*-(α-D-Galactosyl)-2-icosanoylamino-1,3,4-nonanetriol (11d)

^{1}H NMR (400 MHz, Pyr-d_5) δ = 8.42 (d, J = 8.7 Hz, 1H), 6.91 (d, J = 6.4 Hz, 1H), 6.57 (d, J = 4.8 Hz, 1H), 6.49 (t, J = 5.5 Hz, 1H), 6.39 (d, J = 6.1 Hz, 1H), 6.26 (d, J = 3.6 Hz, 1H), 6.03 (d, J = 5.8 Hz, 1H), 5.57 (d, J = 3.9 Hz, 1H), 5.30–5.21 (m, 1H), 4.71–4.61 (m, 2H), 4.55 (br s, 1H), 4.53–4.48 (m, 1H), 4.47–4.35 (m, 4H), 4.34–4.23 (m, 2H), 2.44 (t, J = 7.2 Hz, 2H), 2.30–2.17 (m, 1H), 1.93–1.74 (m, 4H), 1.70–1.56 (m, 1H), 1.41–1.15 (m, 36H), 0.87 (t, J = 6.8 Hz, 3H), 0.81 (t, J = 7.0 Hz, 3H); ^{13}C NMR (101 MHz, Pyr-d_5) δ = 173.3, 101.6, 76.8, 73.1, 72.5, 71.7, 71.0, 70.4, 68.7, 62.7, 51.5, 36.8, 34.4, 32.5, 32.1, 30.0, 30.0, 29.9, 29.9, 29.8, 29.8, 29.6, 26.4, 26.1, 23.0, 23.0, 14.3, 14.3; HRMS (FAB) Calcd for $C_{35}H_{69}NNaO_{9+}$: 670.4865; Found: 670.4880.

4.1.15. (2*S*,3*S*,4*R*)-1-*O*-(α-D-Galactosyl)-2-docosanoylamino-1,3,4-nonanetriol (11e)

^{1}H NMR (400 MHz, Pyr-d_5) δ = 8.42 (d, J = 8.7 Hz, 1H), 6.90 (br s, 1H), 6.57 (d, J = 4.4 Hz, 1H), 6.49 (t, J = 5.3 Hz, 1H), 6.39 (d, J = 5.9 Hz, 1H), 6.26 (d, J = 3.9 Hz, 1H), 6.03 (d, J = 5.5 Hz, 1H), 5.57 (d, J = 3.8 Hz, 1H), 5.31–5.20 (m, 1H), 4.71–4.61 (m, 2H), 4.55 (br s, 1H), 4.53–4.48 (m, 1H), 4.47–4.36 (m, 4H), 4.33–4.24 (m, 2H), 2.44 (t, J = 7.2 Hz, 2H), 2.30–2.18 (m, 1H), 1.93–1.75 (m, 4H), 1.70–1.54 (m, 1H), 1.45–1.11 (m, 40H), 0.87 (t, J = 6.8 Hz, 3H), 0.81 (t, J = 7.0 Hz, 3H); ^{13}C NMR (101 MHz, Pyr-d_5) δ = 173.3, 101.6, 76.8, 73.1, 72.5, 71.7, 71.1, 70.4, 68.7, 62.7, 51.5, 36.8, 34.4, 32.5, 32.1, 30.0, 30.0, 29.9, 29.9, 29.8, 29.8, 29.6, 26.4, 26.1, 23.0, 23.0, 14.3, 14.3; HRMS (FAB) Calcd for $C_{37}H_{73}NNaO_9^+$: 698.5178; Found: 698.5145.

4.1.16. (2*S*,3*S*,4*R*)-1-*O*-(α-D-Galactosyl)-2-tricosanoylamino-1,3,4-nonanetriol (11f)

^{1}H NMR (400 MHz, Pyr-d_5) δ = 8.42 (d, J = 8.5 Hz, 1H), 5.58 (d, J = 3.9 Hz, 1H), 5.30–5.22 (m, 1H), 4.71–4.62 (m, 2H), 4.58–4.54 (m, 1H), 4.54–4.49 (m, 1H), 4.47–4.36 (m, 4H), 4.33–4.25 (m, 2H), 2.44 (t, J = 7.3 Hz, 2H), 2.31–2.18 (m, 1H), 1.94–1.76 (m, 4H), 1.69–1.56 (m, 1H), 1.41–1.18 (m, 42H), 0.87 (t, J = 6.9 Hz, 3H), 0.81 (t, J = 7.2 Hz, 3H); ^{13}C NMR (101 MHz, Pyr-d_5) δ = 101.6, 76.8, 73.1, 72.5, 71.7, 71.0, 70.3, 62.7, 51.5, 36.8, 34.4, 32.5, 32.1, 30.0, 29.9, 29.8, 29.6, 26.4, 26.1, 23.0, 23.0, 14.3, 14.3; HRMS (FAB) Calcd for $C_{38}H_{75}NNaO_9^+$: 712.5334; Found: 712.5302.

4.1.17. (2*S*,3*S*,4*R*)-1-*O*-(α-D-Galactosyl)-2-pentacosanoylamino-1,3,4-nonanetriol (11g)

^{1}H NMR (400 MHz, Pyr-d_5) δ = 8.43 (d, J = 8.7 Hz, 1H), 6.92 (d, J = 4.0 Hz, 1H), 6.58 (d, J = 3.6 Hz, 1H), 6.50 (t, J = 5.3 Hz, 1H), 6.40 (d, J = 6.0 Hz, 1H), 6.27 (d, J = 3.4 Hz, 1H), 6.03 (d, J = 5.6 Hz, 1H), 5.58 (d, J = 3.8 Hz, 1H), 5.32–5.20 (m, 1H), 4.71–4.61 (m, 2H), 4.55 (br s, 1H), 4.54–4.48 (m, 1H), 4.47–4.35 (m, 4H), 4.29 (br s, 2H), 2.44 (t, J = 7.3 Hz, 2H), 2.30–2.18 (m, 1H), 1.94–1.75 (m, 4H), 1.70–1.56 (m, 1H), 1.38–1.20 (m, 46H), 0.87 (t, J = 6.8 Hz, 3H), 0.81 (t, J = 7.1 Hz, 3H); ^{13}C NMR (101 MHz, Pyr-d_5) δ = 173.3, 101.6, 76.8, 73.1, 72.5, 71.7, 71.0, 70.4, 68.7, 62.7, 51.5, 36.8, 34.4, 32.5, 32.1, 30.1, 30.0, 29.9, 29.9, 29.8, 29.8, 29.6, 26.4, 26.1, 23.0, 23.0, 14.3, 14.3; HRMS (FAB) Calcd for $C_{40}H_{79}NNaO_9^+$: 740.5647; Found: 740.5618.

4.1.18. (2*S*,3*S*,4*R*)-1-*O*-(α-D-Galactosyl)-2-hexacosanoylamino-1,3,4-nonanetriol (11h)

^{1}H NMR (400 MHz, Pyr-d_5) δ = 8.43 (d, J = 8.7 Hz, 1H), 6.92 (br s, 1H), 6.58 (br s, 1H), 6.49 (br s, 1H), 6.39 (d, J = 5.9 Hz, 1H), 6.27 (br s, 1H), 6.03 (d, J = 4.5 Hz, 1H), 5.58 (d, J = 3.9 Hz, 1H), 5.30–5.22 (m, 1H), 4.71–4.62 (m, 2H), 4.55 (br s, 1H), 4.54–4.48 (m, 1H), 4.48–4.34 (m, 4H), 4.33–4.24 (m, 2H), 2.44 (t, J = 7.2 Hz, 2H), 2.31–2.18 (m, 1H), 1.94–1.76 (m, 4H), 1.70–1.55 (m, 1H), 1.42–1.16 (m, 48H), 0.87 (t, J = 6.9 Hz, 3H), 0.81 (t, J = 7.1 Hz, 3H); ^{13}C NMR (101 MHz, Pyr-d_5) δ = 173.3, 101.6, 76.8, 73.1, 72.5, 71.7, 71.0, 70.4, 68.7, 62.7, 51.5, 36.8, 34.4, 32.5, 32.1, 30.1, 30.0, 29.9, 29.9, 29.8, 29.8, 29.6, 26.4, 26.1, 23.0, 23.0, 14.3; HRMS (FAB) Calcd for $C_{41}H_{81}NNaO_9^+$: 754.5804; Found: 754.5757.

4.1.19. (2*S*,3*S*,4*R*)-1-*O*-(α-D-Galactosyl)-2-octacosanoylamino-1,3,4-nonanetriol (11i)

^{1}H NMR (400 MHz, Pyr-d_5) δ = 8.42 (d, J = 8.7 Hz, 1H), 6.90 (d, J = 4.1 Hz, 1H), 6.57 (d, J = 4.9 Hz, 1H), 6.49 (t, J = 5.3 Hz, 1H), 6.39 (d, J = 6.1 Hz, 1H), 6.26 (d, J = 3.5 Hz, 1H), 6.02 (d, J = 5.6 Hz, 1H), 5.57 (d, J = 3.9 Hz, 1H), 5.30–5.20 (m, 1H), 4.71–4.61 (m, 2H), 4.57–4.48 (m, 2H), 4.47–4.36 (m, 4H), 4.33–4.25 (m, 2H), 2.44 (t, J = 7.2 Hz, 2H), 2.30–2.19 (m, 1H), 1.93–1.77 (m, 4H), 1.69–1.56 (m, 1H), 1.38–1.22 (m, 52H), 0.87 (t, J = 6.8 Hz, 3H), 0.81 (t, J = 7.1 Hz, 3H); ^{13}C NMR (101 MHz, Pyr-d_5) δ = 173.3, 101.6, 76.8, 73.1, 72.5, 71.7, 71.0, 70.4, 68.7, 62.7, 51.5, 36.8, 34.4, 32.5, 32.1, 30.1, 30.0, 29.9, 29.9, 29.8, 29.8, 29.6, 26.4, 26.1, 23.0, 23.0, 14.3, 14.3; HRMS (FAB) Calcd for $C_{43}H_{85}NNaO_9^+$: 782.6117; Found: 782.6116.

4.1.20. (2*S*,3*S*,4*R*)-1-*O*-(α-D-Galactosyl)-2-tricosanoylamino-1,3,4-decanetriol (11j)

^{1}H NMR (400 MHz, Pyr-d_5) δ = 8.43 (d, J = 8.7 Hz, 1H), 6.92 (d, J = 6.3 Hz, 1H), 6.58 (d, J = 6.0 Hz, 1H), 6.49 (t, J = 5.6 Hz, 1H), 6.40 (d, J = 6.1 Hz, 1H), 6.27 (d, J = 4.0 Hz, 1H), 6.04 (d, J = 5.9 Hz, 1H), 5.58 (d, J = 3.9 Hz, 1H), 5.31–5.21 (m, 1H), 4.71–4.61 (m, 2H), 4.58–4.54 (m, 1H), 4.54–4.49 (m, 1H), 4.47–4.35 (m, 4H), 4.34–4.25 (m, 2H), 2.44 (t, J = 7.2 Hz, 2H), 2.31–2.19 (m, 1H), 1.94–1.75 (m, 4H), 1.70–1.57 (m, 1H), 1.44–1.16 (m, 44H), 0.87 (t, J = 6.8 Hz, 3H), 0.80 (t, J = 7.1 Hz, 3H); ^{13}C NMR (101 MHz, Pyr-d_5) δ = 173.3, 101.6, 76.8, 73.1, 72.5, 71.7, 71.1, 70.4, 68.7, 62.7, 51.5, 36.8, 34.4, 32.2, 32.1, 30.1, 30.0, 29.9, 29.9, 29.8, 29.8, 29.6, 26.4, 23.0, 22.9, 14.3, 14.3; HRMS (FAB) Calcd for $C_{39}H_{77}NNaO_9^+$: 726.5491; Found: 726.5509.

4.1.21. (2*S*,3*S*,4*R*)-5-Cyclopentyl-1-*O*-(α-D-galactosyl)-2-tetracosanoylamino-1,3,4-pentanetriol (11k)

^{1}H NMR (400 MHz, Pyr-d_5) δ = 8.41 (d, J = 8.7 Hz, 1H), 6.91 (d, J = 4.9 Hz, 1H), 6.60 (d, J = 4.3 Hz, 1H), 6.49 (t, J = 5.5 Hz, 1H), 6.37 (d, J = 6.4 Hz, 1H), 6.26 (d, J = 3.9 Hz, 1H), 5.97 (d, J = 6.5 Hz, 1H), 5.57 (d, J = 3.9 Hz, 1H), 5.29–5.19 (m, 1H), 4.71–4.61 (m, 2H), 4.56 (br s, 1H), 4.54–4.49 (m, 1H), 4.47–4.25 (m, 6H), 2.51–2.35 (m, 3H), 2.20–2.11 (m, 1H), 2.01–1.88 (m, 2H), 1.88–1.76 (m, 3H), 1.61–1.49 (m, 2H), 1.49–1.16 (m, 44H), 0.87 (t, J = 6.9 Hz, 3H); ^{13}C NMR (101 MHz, Pyr-d_5) δ = 173.2, 101.6, 77.2, 73.1, 71.7, 71.1, 70.4, 68.7, 62.7, 51.4, 37.3, 36.8, 34.1, 32.4, 32.1, 30.0, 30.0, 29.9, 29.9, 29.8, 29.8, 29.6, 26.4, 25.5, 25.4, 23.0, 14.3; HRMS (FAB) Calcd for $C_{40}H_{77}NNaO_9^+$: 738.5491; Found: 738.5444.

4.1.22. (2*S*,3*S*,4*R*)-1-*O*-(α-D-Galactosyl)-6-phenyl-2-tetracosa noylamino-1,3,4-hexanetriol (11m)

^{1}H NMR (400 MHz, Pyr-d_5) δ = 8.35 (d, J = 8.7 Hz, 1H), 7.38–7.27 (m, 4H), 7.20–7.17 (m, 1H), 7.05 (br s, 1H), 6.59 (br s, 1H), 6.52–6.41 (m, 2H), 6.29 (br s, 1H), 6.22 (d, J = 5.9 Hz, 1H), 5.57 (d, J = 3.8 Hz, 1H), 5.31–5.22 (m, 1H), 4.69–4.59 (m, 2H), 4.56 (br s, 1H), 4.48–4.25 (m, 7H), 3.21 (ddd, J = 4.5, 9.8, 13.9 Hz, 1H), 3.00 (ddd, J = 6.8, 9.7, 13.5 Hz, 1H), 2.66–2.55 (m, 1H), 2.47–2.33 (m, 2H), 2.23–2.10 (m, 1H), 1.80 (quin, J = 7.6 Hz, 2H), 1.40–1.14 (m, 40H), 0.87 (t, J = 6.9 Hz, 3H); ^{13}C NMR (101 MHz, Pyr-d_5) δ = 173.2, 143.6, 129.1, 128.7, 125.9, 101.5, 76.8, 73.0, 71.7, 71.6, 71.0, 70.3, 68.4, 62.7, 51.3, 36.8, 36.5, 32.7, 32.1, 30.0, 29.9, 29.9, 29.8, 29.8, 29.6, 26.4, 23.0, 14.3; HRMS (FAB) Calcd for $C_{42}H_{75}NNaO_9^+$: 760.5334; Found: 760.5322.

4.1.23. (2*S*,3*S*,4*R*)-1-*O*-(α-D-Galactosyl)-5-(*p*-tolyl)-2-tetracosano ylamino-1,3,4-pentanetriol (11n)

^{1}H NMR (400 MHz, Pyr-d_5) δ = 8.51 (d, J = 8.5 Hz, 1H), 7.51 (d, J = 8.0 Hz, 2H), 7.08 (d, J = 7.7 Hz, 2H), 6.92–6.12 (m, 6H), 5.52 (d, J = 4.0 Hz, 1H), 5.28 (qd, J = 4.7, 8.9 Hz, 1H), 4.71–4.58 (m, 2H), 4.58–4.47 (m, 3H), 4.47–4.30 (m, 5H), 3.67 (dd, J = 1.8, 13.5 Hz, 1H), 3.12 (dd, J = 9.2, 13.8 Hz, 1H), 2.43 (dt, J = 3.3, 7.5 Hz, 2H), 2.21 (s, 3H), 1.81 (quin, J = 7.6 Hz, 2H), 1.43–1.10 (m, 40H), 0.87 (t, J = 6.8 Hz, 3H); ^{13}C NMR (101 MHz, Pyr-d_5) δ = 173.4, 138.2, 130.3, 129.1, 101.8, 76.5, 74.1, 73.1, 71.6, 71.0, 70.4, 69.2, 62.7, 51.7, 36.8, 32.1, 30.1, 30.0, 29.9, 29.9, 29.8, 29.8, 29.6, 26.4, 23.0, 21.0, 14.3; HRMS (FAB) Calcd for $C_{42}H_{75}NNaO_9^+$: 760.5334; Found: 760.5358.

4.1.24. (2*S*,3*S*,4*R*)-1-*O*-(α-D-Galactosyl)-6-oxa-2-tetracosanoy lamino-1,3,4-heptanetriol (11o)

^{1}H NMR (400 MHz, Pyr-d_5) δ = 8.47 (d, J = 8.7 Hz, 1H), 5.54 (d, J = 3.9 Hz, 1H), 5.30–5.22 (m, 1H), 4.69–4.61 (m, 2H), 4.57–4.47 (m, 3H), 4.46–4.33 (m, 5H), 4.07 (dd, J = 2.7, 9.9 Hz, 1H), 3.94 (dd, J = 6.1, 9.8 Hz, 1H), 3.35 (s, 3H), 2.42 (dt, J = 1.5, 7.5 Hz, 2H), 1.79 (quin, J = 7.5 Hz, 2H), 1.38–1.14 (m, 40H), 0.87 (t, J = 7.0 Hz, 3H); ^{13}C NMR (101 MHz, Pyr-d_5) δ = 173.4, 101.6, 76.0, 74.0, 73.1, 72.0, 71.6, 71.0, 70.3, 68.5, 62.7, 59.0, 51.5, 36.8, 32.1, 30.0, 30.0, 29.9, 29.9, 29.8, 29.8, 29.6, 26.4, 23.0, 14.3; HRMS (FAB) Calcd for $C_{36}H_{71}NNaO_{10}^+$: 700.4970; Found: 700.4920.

4.1.25. (2*S*,3*S*,4*R*)-1-*O*-(α-D-Galactosyl)-6-oxa-2-tetracosanoy lamino-1,3,4-octadecanetriol (11q)

^{1}H NMR (400 MHz, Pyr-d_5) δ = 8.47 (d, J = 8.7 Hz, 1H), 6.86 (br s, 1H), 6.62–6.42 (m, 3H), 6.36 (d, J = 6.3 Hz, 1H), 6.28 (br s, 1H), 5.54 (d, J = 3.8 Hz, 1H), 5.31–5.22 (m, 1H), 4.71–4.60 (m, 2H), 4.58–4.33 (m, 8H), 4.17 (dd, J = 2.6, 9.9 Hz, 1H), 4.04 (dd, J = 6.1, 9.9 Hz, 1H), 3.62–3.49 (m, 2H), 2.43 (dt, J = 1.6, 7.5 Hz, 2H), 1.80 (quin, J = 7.6 Hz, 2H), 1.64–1.55 (m, 2H), 1.40–1.16 (m, 58H), 0.90–0.85 (m, 6H); ^{13}C NMR (101 MHz, Pyr-d_5) δ = 173.4, 101.6, 74.3, 74.1, 73.1, 72.1, 71.9, 71.7, 71.0, 70.4, 68.7, 62.7, 51.6, 36.8, 32.2, 30.3, 30.1, 30.0, 29.9, 29.9, 29.8, 29.8, 29.6, 26.6, 26.4, 23.0, 14.3; HRMS (FAB) Calcd for $C_{47}H_{93}NNaO_{10}^+$: 854.6692; Found: 854.6697.

4.1.26. (2*S*,3*S*,4*R*)-1-*O*-(α-D-Galactosyl)-5-phenoxy-2-tetracosa noylamino-1,3,4-pentanetriol (11r)

^{1}H NMR (400 MHz, Pyr-d_5) δ = 8.56 (d, J = 8.7 Hz, 1H), 7.29–7.23 (m, 2H), 7.09–7.03 (m, 2H), 6.96–6.91 (m, 1H), 6.70 (br s, 1H), 5.56 (d, J = 3.8 Hz, 1H), 5.37–5.30 (m, 1H), 4.77–4.58 (m, 5H), 4.58–4.49 (m, 3H), 4.47–4.35 (m, 4H), 2.44 (dt, J = 2.1, 7.5 Hz, 2H), 1.80 (quin, J = 7.6 Hz, 2H), 1.38–1.17 (m, 40H), 0.87 (t, J = 6.9 Hz, 3H); ^{13}C NMR (101 MHz, Pyr-d_5) δ = 173.5, 160.1, 129.8, 120.8, 115.2, 101.6, 73.7, 73.1, 71.7, 71.6, 71.4, 71.0, 70.3, 68.6, 62.7, 51.5, 36.8, 32.1, 30.0, 30.0, 29.9, 29.9, 29.8, 29.8, 29.6, 26.4, 23.0, 14.3; HRMS (FAB) Calcd for $C_{41}H_{73}NNaO_{10}^+$: 762.5127; Found: 762.5139.

4.1.27. (3*R*,4*S*,5*R*)-4,5-*O*-Isopropylidene-1-(2,3,4,6-tetra-*O*-benzyl-α-D-galactosyl)-1-decyne-3,4,5-triol (14)

To a solution of **12** (92.7 mg, 0.17 mmol) in THF (2 ml) was added dropwise a solution of 1.57 M *n*-BuLi in hexane (120 μl, 0.19 mmol) at −45 °C, and the reaction temperature was raised to 0 °C. After 30 min of stirring the mixture was cooled to −48 °C and a solution of **13** (117 mg, 0.584 mmol) in THF (1.5 ml) was added. After 90 min of stirring the mixture was allowed to gradually warm to −30 °C. The mixture was quenched with 0.1 M phosphonate buffer (2 ml, pH 7.4) at −30 °C and allowed to warm to rt. Satd NaCl aq (5 ml) and water (40 ml) was added, and the product was extracted with EtOAc (40 ml × 1, 30 ml × 2). Combined organic layer was dried over Na_2SO_4, concentrated and purified by silica gel column chromatography (hexane/EtOAc; 9–25%) to yield **14** as a pale yellow oil (43.7 mg, 35% (47% based on recovered starting material)), along with its epimer (27.9 mg, 22% (30% br sm)) and recovered **12** (24.5 mg, 26%). ^{1}H NMR (400 MHz, $CDCl_3$) δ = 7.38–7.21 (m, 20H), 4.91 (d, J = 11.4 Hz, 1H), 4.86 (dd, J = 1.6, 5.7 Hz, 1H), 4.81 (d, J = 11.8 Hz, 1H), 4.74 (d, J = 11.8 Hz, 1H), 4.73 (d, J = 11.8 Hz, 1H), 4.67 (d, J = 11.8 Hz, 1H), 4.55 (d, J = 11.4 Hz, 1H), 4.48 (d, J = 12.2 Hz, 1H), 4.40 (d, J = 11.8 Hz, 1H), 4.38–4.33 (m, 1H), 4.15–4.04 (m, 4H), 3.96 (d, J = 1.6 Hz, 1H), 3.82 (dd, J = 2.8, 10.1 Hz, 1H), 3.55–3.49 (m, 2H), 2.65 (d, J = 3.7 Hz, 1H), 1.47 (s, 3H), 1.69–1.41 (m, 3H), 1.37 (s, 3H), 1.30–1.19 (m, 5H), 0.82 (t, J = 6.9 Hz, 3H); MS (FAB) 749 $(M+H)^+$.

4.1.28. (3*R*,4*R*,5*R*)-4,5-*O*-Isopropylidene-3-*O*-methanesulfonyl-1-(2,3,4,6-tetra-*O*-benzyl-α-D-galactosyl)-3,4,5-decanetriol (15)

To a warmed solution of **14** (15.6 mg, 0.021 mmol) and *p*-toluenesulfonylhydrazine (38.8 mg, 0.208 mmol) in dimethoxyethane was added 1 N NaOAc aq solution in 10 portions over 5 h. The mixture was stirred at 85 °C for 4.5 h after the final addition. After cooling to rt, the reaction was diluted with water (10 ml) and extracted with CH_2Cl_2 (30 ml × 1, 20 ml × 1, 10 ml × 1). Combined organic layers was dried over Na_2SO_4, concentrated and purified by silica gel column chromatography (hexane/EtOAc; 25%) to yield saturated alcohol as a colorless oil (14.2 mg, 91%). The alcohol was

dissolved in CH_2Cl_2 (1 ml) and pyridine (0.5 ml), and to the solution was added methanesulfonyl chloride (four drops) at 0 °C. After overnight stirring at rt the reaction was diluted with EtOAc (30 ml) and washed with satd NH_4Cl aq (20 ml) and water (10 ml). The organic layer was dried over Na_2SO_4, concentrated and purified over silica gel column chromatography (hexane/EtOAc; 25%) to yield compound **15** as a colorless oil (14.7 mg, 94%). ^1H NMR (400 MHz, $CDCl_3$) δ = 7.35–7.22 (m, 20H), 4.78–4.70 (m, 2H), 4.68 (s, 2H), 4.60 (s, 2H), 4.55 (d, J = 11.8 Hz, 1H), 4.49 (d, J = 11.4 Hz, 1H), 4.43 (d, J = 11.8 Hz, 1H), 4.11–4.04 (m, 2H), 3.99–3.92 (m, 2H), 3.88 (br s, 2H), 3.77–3.70 (m, 2H), 3.56 (dd, J = 4.7, 10.3 Hz, 1H), 3.08 (s, 3H), 1.97–1.46 (m, 5H), 1.44 (s, 3H), 1.33 (s, 3H), 1.32–1.22 (m, 7H), 0.88 (t, J = 6.9 Hz, 3H); MS (FAB) 831 $(M+H)^+$.

4.1.29. (3*S*,4*S*,5*R*)-4,5-*O*-Isopropylidene-1-(2,3,4,6-tetra-*O*-benzyl-α-D-galactosyl)-3-tetracosanoylamino-4,5-decanediol (16)

To a solution of **15** (14.7 mg, 0.0177 mmol) in DMF (1 ml) was added NaN_3 (18.0 mg, 0.277 mmol) at 0 °C, and the mixture was stirred at 90 °C for 17 h. After cooling to rt the mixture was diluted with EtOAc (50 ml), washed with water (30 ml × 3), dried over Na_2SO_4, concentrated and passed through silica gel column to give the crude azide. The crude azide was stirred overnight with Lindlar catalyst (14.6 mg) in EtOH (2 ml) under H_2 atmosphere. Insolubles were removed by passing through membrane filter, and the filtrate was concentrated to give amine as a pale yellow oil. A mixture of this amine, Lignoceric acid (11.7 mg, 0.0317 mmol), 1-hydroxy-7-azabenzotriazole (5.8 mg, 0.0426 mmol), Et_3N (3 drops), and 1-ethyl-3-(3-dimethylaminopropyl) carbodiimide hydrochloride (9.0 mg, 0.0469 mmol) in DMF (1 ml) and CH_2Cl_2 (1 ml) was stirred overnight at rt. The reaction was diluted with EtOAc (40 ml) and washed with satd $NaHCO_3$ aq (30 ml) and water (30 ml). The organic layer was dried over Na_2SO_4, concentrated and purified by silica gel column chromatography (hexane/EtOAc; 17% to 20%) to yield **16** as a colorless solid (9.3 mg, 48%). ^1H NMR (400 MHz, $CDCl_3$) δ = 7.35–7.22 (m, 20H), 5.68 (d, J = 8.9 Hz, 1H), 4.74 (d, J = 11.4 Hz, 1H), 4.68 (d, J = 12.2 Hz, 1H), 4.64 (d, J = 11.8 Hz, 1H), 4.63 (d, J = 11.8 Hz, 1H), 4.57–4.48 (m, 3H), 4.45 (d, J = 11.8 Hz, 1H), 4.06–3.99 (m, 2H), 3.99–3.92 (m, 4H), 3.87–3.74 (m, 2H), 3.68 (dd, J = 2.4, 7.7 Hz, 1H), 3.54 (dd, J = 4.3, 10.3 Hz, 1H), 2.10–1.99 (m, 2H), 1.40 (s, 3H), 1.30 (s, 3H), 1.83–1.13 (m, 54H), 0.88 (t, J = 6.5 Hz, 3H), 0.86 (t, J = 6.5 Hz, 3H); MS (FAB) 1103 $(M+H)^+$.

4.1.30. (3*S*,4*S*,5*R*)-1-(α-D-Galactopyranosyl)-3-tetracosanoylamino-4,5-decanediol (4)

A mixture of **16** in 80% AcOH was stirred at 60 °C for 3 h, after which all of the volatiles were removed and the residue was purified by silica gel column chromatography (hexane/EtOAc; 33% to 50%) to yield diol as a colorless solid (7.9 mg, 88%). A mixture of this diol and Pearlman's catalyst (10.6 mg) in MeOH (2.5 ml) and CH_2Cl_2 (1 ml) was stirred under H_2 atmosphere for 4.5 h. Insolubles were removed by passing through membrane filter, and washed thoroughly with mixed solution of MeOH and CH_2Cl_2. The filtrate was concentrated to give compound **4** as a colorless solid (5.4 mg, quant.). ^1H NMR (400 MHz, Pyr-d_5) δ = 8.41 (d, J = 9.0 Hz, 1H), 6.81–5.71 (m, 6H), 5.17–5.07 (m, 1H), 4.72 (dd, J = 5.5, 8.9 Hz, 1H), 4.57–4.45 (m, 3H), 4.36 (dd, J = 4.6, 11.2 Hz, 1H), 4.29–4.11 (m, 4H), 2.78–2.65 (m, 1H), 2.65–2.53 (m, 1H), 2.53–2.38 (m, 2H), 2.38–2.13 (m, 3H), 1.97–1.76 (m, 4H), 1.74–1.57 (m, 1H), 1.49–1.09 (m, 44H), 0.87 (t, J = 6.8 Hz, 3H), 0.81 (t, J = 7.2 Hz, 3H); ^{13}C NMR (101 MHz, Pyr-d_5) δ = 173.4, 78.5, 77.0, 73.8, 72.7, 72.2, 70.6, 70.4, 62.8, 52.7, 37.0, 34.5, 32.5, 32.1, 30.1, 30.0, 29.9, 29.9, 29.8, 29.6, 26.6, 26.2, 23.1, 23.0, 14.3; HRMS (FAB) Calcd for $C_{40}H_{79}NNaO_8^+$: 724.5698; Found: 724.5693.

4.2. Biological evaluation

4.2.1. In vitro cytokine production

Splenocytes were prepared from the spleens of C57BL/6 mice (6–8 weeks old, female) and suspended in a RPMI1640 medium (purchased from Nacalai) containing 10% fetal bovine serum (purchased from GIBCO), 5×10^{-5} M 2-mercaptoethanol (purchased from GIBCO), 1 mM pyruvate (purchased from SIGMA), and 25 mM HEPES (purchased from SIGMA). The cells (5×10^5 cells/well) were stimulated with glycolipid derivatives at a concentration of 100 ng/ml for 72 h at 37 °C in a 96-well flat bottom plate (purchased from IWAKI), and the concentration of IL-4 and IFN-γ in the culture supernatant were measured by ELISA (BD Pharmingen EIA Kit). Compound **2** was always included in the assay as a control and the cytokine release were expressed as relative to that of **2** for the mean of at least three experiments.

4.2.2. In vivo cytokine production

Each glycolipid was dissolved in 0.5% DMSO in saline. To clarify the antagonist activity of **4**, the compound was injected intravenously into C57BL/6 mice (9 weeks old, female) though tail vein at 0.1 μg/mouse, 15 min before OCH injection (0.1 μg/mouse). 3, 6, 9 h after second injection, sera were collected, and the content of serum IL-4 and IFN-γ were measured by ELISA (BioLegend ELISA Set). The data were presented as mean ± SD (N = 4–5). Statistical analysis was performed by Student's t-test by using JMP9.0.2 (SAS Institute Inc., Cary, NC).

4.2.3. In silico optimization of 2/hCD1d complex

Both acyl and phytosphingosine chain of **1** bound to hCD1d in the crystal structure was truncated in silico to correspond to **2**, and the complex thus obtained was further optimized. Optimization of the complex was performed stepwise as follows, utilizing Macromodel Ver. 9.0[26] [force field OPLS2005/solv. Water] (convergence threshold .05 kJ/mol/Å): (i) main chain, Asp80, Asp151, Thr154 and ligand fixed, (ii) main chain, Asp80(Oδ1, Oδ2), Asp151(Oδ1, Oδ2), Thr154(Oγ) and oxygen atoms of the ligand fixed, (iii) main chain, distances among selected ligand atoms and Asp80, Asp151, Thr154 fixed, (iv) main chain fixed, (v) optimization of all the atoms.

Acknowledgements

Authors thank Dr. Y. Tanaka, Dr. K. Yamaoka-Kadoshima, Ms. F. Nakanishi-Izumi, and Ms. M. Nakajima-Komori for performing cytokine assays. Dr. T. Nishihara is acknowledged for support and encouragement throughout this study.

References and notes

1. For recent reviews: (a) Joyce, S.; Girardi, E.; Zajonc, D. M. *J. Immunol.* **2011**, *187*, 1081; (b) Venkataswamya, M. M.; Porcelli, S. A. *Semin. Immunol.* **2010**, *22*, 68; (c) Van Kaer, L. *Immunol. Res.* **2004**, *30*, 139; (d) Wu, L.; Gabriel, C. L.; Parekh, W.; Van Kaer, L. *Tissue Antigens* **2009**, *73*, 535; (e) Cohen, N. R.; Garq, S.; Brenner, M. B. *Adv. Immunol.* **2009**, *102*, 1.
2. (a) Wu, D.; Xing, G.-W.; Poles, M. A.; Horowitz, A.; Kinjo, Y.; Sullivan, B.; Bodmer-Narkevitch, V.; Plettenburg, O.; Kronenberg, M.; Tsuji, M.; Ho, D. D. *Proc. Natl. Acad. Sci. U.S.A.* **2005**, *102*, 1351; (b) Zajonc, D. M.; Kronenberg, M. *Immunol. Rev.* **2009**, *230*, 188.
3. Zhou, D.; Mattner, J.; Cantu, C., III; Schrantz, N.; Yin, N.; Gao, Y.; Sagiv, Y.; Hudspeth, K.; Wu, Y.-P.; Yamashita, T.; Teneberg, S.; Wang, D.; Proia, R. L.; Levery, S. B.; Savage, P. B.; Teyton, L.; Bendelac, A. *Science* **2004**, *306*, 1786.
4. Wu, D.; Fujio, M.; Wong, C.-H. *Bioorg. Med. Chem.* **2008**, *16*, 1073.
5. (a) Morita, M.; Motoki, K.; Akimoto, K.; Natori, T.; Sakai, T.; Sawa, E.; Yamaji, K.; Koezuka, Y.; Kobayashi, E.; Fukushima, H. *J. Med. Chem.* **1995**, *38*, 2176; (b) Morita, M.; Sawa, E.; Yamaji, K.; Sakai, T.; Natori, T.; Koezuka, Y.; Fukushima, H.; Akimoto, K. *Biosci., Biotechnol., Biochem.* **1996**, *60*, 288; (c) Takikawa, H.; Muto, S.; Mori, K. *Tetrahedron* **1998**, *54*, 3141; (d) Graziani, A.; Passacantilli, P.; Piancatelli, G.; Tani, S. *Tetrahedron: Asymmetry* **2000**, *11*, 3921.
6. Yu, K. O. A.; Porcelli, S. A. *Immunol. Lett.* **2005**, *100*, 42. and references cited therein.

7. Liang, P.-H.; Imamura, M.; Li, X.; Wu, D.; Fujio, M.; Guy, R. T.; Wu, B.-C.; Tsuji, M.; Wong, C.-H. *J. Am. Chem. Soc.* **2008**, *130*, 12348.
8. (a) Yang, G.; Schmieg, J.; Tsuji, M.; Franck, R. W. *Angew. Chem., Int. Ed.* **2004**, *43*, 3818; (b) Schmieg, J.; Yang, G.; Franck, R. W.; Tsuji, M. *J. Exp. Med.* **2003**, *198*, 1631.
9. (a) Miyamoto, K.; Miyake, S.; Yamamura, T. *Nature* **2001**, *413*, 531; (b) Yamamura, T.; Miyake, S. PCT Int. Appl. WO 2003/016326, 2003; *Chem. Abstr.* **2003**, *138*, 205292m.; (c) Yamamura, T.; Miyamoto, K.; Illes, Z.; Pal, E.; Araki, M.; Miyake, S. *Curr. Top. Med. Chem.* **2004**, *4*, 561; (d) Oki, S.; Chiba, A.; Yamamura, T.; Miyake, S. *J. Clin. Invest.* **2004**, *113*, 1631.
10. Chiba, A.; Oki, S.; Miyamoto, K.; Hashimoto, H.; Yamamura, T.; Miyake, S. *Arthritis Rheum.* **2004**, *50*, 305.
11. Borg, N. A.; Wun, K. S.; Kjer-Nielsen, L.; Wilce, M. C. J.; Pellicci, D. G.; Koh, R.; Besra, G. S.; Bharadwaj, M.; Godfrey, D. I.; McCluskey, J.; Rossjohn, J. *Nature* **2007**, *448*, 44.
12. Koch, M.; Stronge, V. S.; Shepherd, D.; Gadola, S. D.; Mathew, B.; Ritter, G.; Fersht, A. R.; Besra, G. S.; Schmidt, R. R.; Jones, E. Y.; Cerundolo, V. *Nat. Immunol.* **2005**, *6*, 819.
13. Henon, E.; Dauchez, M.; Haudrechy, A.; Banchet, A. *Tetrahedron* **2008**, *64*, 9480.
14. McCarthy, C.; Shepherd, D.; Fleire, S.; Stronge, V. S.; Koch, M.; Illarinov, P. A.; Bossi, G.; Salio, M.; Denkberg, G.; Reddington, F.; Tarlton, A.; Reddy, B. G.; van der Merwe, P. A.; Bersa, G. S.; Jones, W. Y.; Bartisa, F. D.; Cerundolo, V. *J. Exp. Med.* **2007**, *204*, 1131.
15. Murata, K.; Toba, T.; Nakanishi, K.; Takahashi, B.; Yamamura, T.; Miyake, S.; Annoura, H. *J. Org. Chem.* **2005**, *70*, 2398.
16. Toba, T.; Murata, K.; Nakanishi, K.; Takahashi, B.; Takemoto, N.; Akabane, M.; Nakatsuka, T.; Imajo, S.; Yamamura, T.; Miyake, S.; Annoura, H. *Bioorg. Med. Chem. Lett.* **2007**, *17*, 2781.
17. Schmidt, R. R.; Maier, T. *Carbohydr. Res.* **1988**, *174*, 169.
18. The anomeric diastereomers were separable by column chromatography over silica gel. The stereochemistry of the galactoside linkage was determined by ^{1}H NMR spectra. The anomeric proton of the α-isomer appears more downfield than β-isomer (typically ~0.5 ppm) and shows smaller coupling constant (typically less than 5 Hz). Example data of the anomeric proton (400 MHz, $CDCl_3$): For the α-isomer **9** (R = *n*-Bu): δ 4.94 (d, J = 3.5 Hz, 1H), and its corresponding β-isomer: δ 4.41 (d, J = 7.7 Hz, 1H).
19. Taniguchi, M.; Kawano, T.; Koezuka, Y. PCT Int. Appl. WO1998/044928A, 1998, 129, 310889.
20. Toba, T.; Murata, K.; Yamamura, T.; Miyake, S.; Annoura, H. *Tetrahedron Lett.* **2005**, *46*, 5043.
21. Dondoni, A.; Mariotti, G.; Marra, A. *J. Org. Chem.* **2002**, 67, 4475.
22. Ohtani, I.; Kusumi, T.; Kashman, Y.; Kakisawa, H. *J. Am. Chem. Soc.* **1991**, *113*, 4092–4096.
23. Annoura, H.; Murata, K.; Yamamura, T. PCT Int. Appl. WO2004/072091, 2004; *Chem. Abstr.* **2004**, *141*, 225769n.
24. Michieletti, M.; Bracci, A.; Compostella, F.; De Libero, G.; Mori, L.; Fallarini, S.; Lombardi, G.; Pnaza, L. *J. Org. Chem.* **2008**, *73*, 9192.
25. MAESTRO *Ver. 7.5.112*; Schrödinger, LLC: New York.
26. Macromodel Ver. 9.0 (Schrödinger, LLC): Mohamadi, F.; Richards, N. G. J.; Guida, W. C.; Liskcamp, R.; Lipton, M.; Caufield, C.; Chang, G.; Hendrickson, T.; Still, W. C. *J. Comput. Chem.* **1990**, *11*, 440.

Chiba et al. Arthritis Research & Therapy 2012, 14:R9
http://arthritis-research.com/content/14/1/R9

arthritis research&therapy

RESEARCH ARTICLE Open Access

A 4-trifluoromethyl analogue of celecoxib inhibits arthritis by suppressing innate immune cell activation

Asako Chiba[1], Miho Mizuno[1], Chiharu Tomi[1], Ryohsuke Tajima[1], Iraide Alloza[2], Alessandra di Penta[2], Takashi Yamamura[1], Koen Vandenbroeck[2,3] and Sachiko Miyake[1*]

Abstract

Introduction: Celecoxib, a highly specific cyclooxygenase-2 (COX-2) inhibitor has been reported to have COX-2-independent immunomodulatory effects. However, celecoxib itself has only mild suppressive effects on arthritis. Recently, we reported that a 4-trifluoromethyl analogue of celecoxib (TFM-C) with 205-fold lower COX-2-inhibitory activity inhibits secretion of IL-12 family cytokines through a COX-2-independent mechanism that involves Ca^{2+}-mediated intracellular retention of the IL-12 polypeptide chains. In this study, we explored the capacity of TFM-C as a new therapeutic agent for arthritis.

Methods: To induce collagen-induced arthritis (CIA), DBA1/J mice were immunized with bovine type II collagen (CII) in Freund's adjuvant. Collagen antibody-induced arthritis (CAIA) was induced in C57BL/6 mice by injecting anti-CII antibodies. Mice received 10 μg/g of TFM-C or celecoxib every other day. The effects of TFM-C on clinical and histopathological severities were assessed. The serum levels of CII-specific antibodies were measured by ELISA. The effects of TFM-C on mast cell activation, cytokine producing capacity by macophages, and neutrophil recruitment were also evaluated.

Results: TFM-C inhibited the severity of CIA and CAIA more strongly than celecoxib. TFM-C treatments had little effect on CII-specific antibody levels in serum. TFM-C suppressed the activation of mast cells in arthritic joints. TFM-C also suppressed the production of inflammatory cytokines by macrophages and leukocyte influx in thioglycollate-induced peritonitis.

Conclusion: These results indicate that TFM-C may serve as an effective new disease-modifying drug for treatment of arthritis, such as rheumatoid arthritis.

Introduction

In the past decade, a series of potent new biologic therapeutics have demonstrated remarkable clinical efficacy in several autoimmune diseases, including rheumatoid arthritis (RA). In the case of RA, a chronic progressive autoimmune disease that targets joints and occurs in approximately 0.5 to 1% of adults, biologic agents, such as TNF inhibitors, have proven effective in patients not responding to disease-modifying anti-rheumatic drugs, such as methotrexate. However, about 30% of patients treated with a TNF inhibitor are primary non-responders. Moreover, a substantial proportion of patients experience a loss of efficacy after a primary response to a TNF inhibitor (secondary non-responders) [1-3]. More recently, as new therapies have become available, including biological agents targeting IL-6, B cells and T cells, it has become clear that a notable proportion of patients respond to these new biological agents even among primary and secondary non-responders to TNF inhibitors [3-10]. These individual differences in response to each agent highlight the difficulty and limit of treating multifactorial disease by targeting single cytokine or single cell type. Patient-tailored therapy might be able to

* Correspondence: miyake@ncnp.go.jp
[1]Department of Immunology, National Institute of Neuroscience, National Center of Neurology and Psychiatry, 4-1-1 Ogawahigashi, Kodaira, Tokyo 187-8502, Japan
Full list of author information is available at the end of the article

overcome this issue, but good biomarkers to predict treatment responses have not yet been elucidated.

Therefore, as described above, biological drugs have limited values. In addition, such drugs may be accompanied by serious side effects [11,12]. Furthermore, the high cost of these biological drugs may make access to these reagents prohibitive for the general public. Alternative therapeutic options, such as small molecule-based drugs, continue to be an important challenge.

The involvement of prostaglandin pathways in the pathogenesis of arthritis has been shown in animal models by using mice lacking genes, such as cycolooxygenase-2 (COX-2), prostaglandin E synthase, or prostacyclin receptor [13-15]. As COX-2 knockout mice normally develop autoreactive T cells in collagen-induced arthritis (CIA) [13], prostaglandin pathways appear to be involved mainly in the effector phase of arthritis. However, treatment with celecoxib, a prototype drug belonging to a new generation of highly specific COX-2 inhibitors has been reported to have only mild suppressive effects on animal models of arthritis, and strong inhibition of arthritis was achieved only when mice were treated in the combination of celecoxib with leukotriene inhibitors [16-19]. In humans, although celecoxib is widely used as an analgesic agent in patients with RA or osteoarthritis, there is no evidence that celecoxib therapy modulates the clinical course of RA. In addition, recently it has been shown that celecoxib enhances TNFα production by RA synovial membrane cultures and human monocytes [20].

Celecoxib has been reported to exhibit COX-2-independent effects, such as tumor growth inhibition and immunomodulation [21,22]. Previously, we demonstrated that celecoxib treatment suppressed experimental autoimmune encephalomyelitis (EAE) in a COX-2 independent manner [22]. We recently developed a trifluoromethyl analogue of celecoxib (TFM-C; full name: 4-[5-(4-trifluoromethylphenyl)-3-(trifluoromet-hyl)-1*H*-pyrazol-1-yl]benzenesulfonamide), with 205-fold lower COX-2-inhibitory activity. In studies using recombinant cell lines, TFM-C inhibited secretion of the IL-12 family cytokines, IL-12, p80 and IL-23, through a COX-2-independent, Ca^{2+}-dependent mechanism involving chaperone-mediated cytokine retention in the endoplasmic reticulum coupled to degradation via the ER stress protein HERP [23,24]. In the present study, we demonstrate that TFM-C inhibits innate immune cells and animal models of arthritis, including CIA and type II collagen antibody-induced arthritis (CAIA), in contrast to the limited inhibitory effect of celecoxib. TFM-C suppresses the activation of mast cells in arthritic joints. Moreover, TFM-C treatment suppresses the production of inflammatory cytokines by macrophages and leukocyte recruitment. These findings indicate that TFM-C may serve as an effective new drug for the treatment of arthritis, including RA.

Materials and methods

Differentiation and stimulation of U937 cells

Human U937 cells were obtained from the American Type Culture Collection (Rockville, MD, USA) and cultured in RPMI 1640 supplemented with 10% FCS. To differentiate U937 cells, 5×10^5 cells were treated with PMA (25 ng/ml) for 24 hours. At 22 hours of PMA treatment, 50 μM of TFM-C was added for 2 hours. Subsequently, cells were stimulated with 5 μg/ml of LPS and PMA (25 ng/ml) for 0, 3, 6, 12 and 24 hours in the presence or absence of TFM-C. Supernatants were harvested and assayed for cytokine production by means of Quansys Q-Plex™ Array (Quansys Bioscience, Logan, Utah, USA). RNA isolation was performed following the manufacturer's instructions (Macherey-Nagel, Düren, Germany).

Quantitative RT-PCR (qPCR)

A total of 200 ng of RNA extracted from U937 cells was retrotranscribed to cDNA using random primers according to the manufacturer's protocol (Applied Biosystems, Carlsbad, California, USA). qPCR was performed with the Supermix for SsoFast EvaGreen (Biorad, Hercules, California, USA) on a 7500 Fast Real-Time PCR System (Applied Biosystems). For each target gene, qPCR QuantiTect Primer Assays were used (Qiagen Hilden, Germany). For each sample, expression levels of the transcripts of interest were compared to that of endogenous GAPDH. The levels of mRNA are calculated as 2^{-Ct}.

Quansys Q-Plex™ Array chemiluminescent

A total of 30 μl of medium from differentiated U937 cells treated with PMA/LPS/TFM-C or LPS/PMA were analyzed. Human Cytokine Stripwells (16-plex) were used following the manufacturer's instructions. The image was acquired using Bio-Rad Chemidoc camera and analyzed with Q-View Software (Quansys Bioscience, Logan, Utah, USA)

DAPI staining

Differentiated U937s were treated with LPS/PMA/TFM-C for 6, 12 and 24 hours and then fixed with 2% PFA. The cells were washed three times with PBS and then incubated with DAPI (1:50000; Molecular Probes, Carlsbad, California, USA) in PBS. Coverslips were embedded in Fluoro-Gel (Electron Microscopy Science, Hatfield, Pennsylvania, USA). Images were recorded using the ApoTome system (AxioVision, Carl Zeiss, Inc., Oberkochen, Germany) and analyzed using the ImageJ program (version 1.40, Bethesda, Maryland, USA).

AlarmBlue staining of U937 cells

The number of viable cells was tested at 6, 12, and 24 hours after TFM-C exposure by adding the AlamarBlue reagent (AbD Serotec, Cambridge, UK). Absorbance was measured at wavelengths of 570 nm and 600 nm after required incubation, using a Varioskan Flash (Thermo Fisher Scientific, Fremont, CA, USA). Absorbance values of samples were normalized with values of the cell culture media without cells. The results are presented as the proportion of viable cells, calculated by dividing the absorbance values of drug-treated samples by the absorbance values of untreated control samples.

Mice

DBA1/J mice were purchased from Oriental Yeast Co., Ltd. (Tokyo, Japan). C57BL/6J (B6) mice were purchased from CLEA Laboratory Animal Corp. (Tokyo, Japan). Animal care and use were in accordance with institutional guidelines and all animal experiments were approved by the Institutional Animal Care and Use Committee of the National Institute of Neuroscience.

Induction of CIA

DBA1/J male mice (n = 5 to 6 per group, 7 to 8 weeks old) were immunized intradermally at the base of the tail with 150 μg of bovine type II collagen (CII) (Collagen Research Center, Tokyo, Japan) emulsified with an equal volume of complete Freund's adjuvant (CFA), containing 250 μg of H37Ra *Mycobacterium tuberculosis (Mtb)* (Difco, Detroit, MI, USA). DBA1/J mice were boosted 21 days after immunization by intradermal injection with 150 μg of CII emulsified with incomplete Freund's adjuvant (IFA).

Induction of CAIA

B6 female mice (n = 5 to 6 per group, 7 to 8 weeks old) were injected intravenously with 2 mg of a mixture of anti-CII monoclonal antibodies (mAbs) (Arthrogen-CIA mAb (Chondrex. LLC. Seattle, WA, USA)), and two days later with 50 μg of lipopolysaccharide (LPS) was injected intraperitoneally.

Clinical assessment of arthritis

Mice were examined for signs of joint inflammation and scored as follows: 0: no change, 1: significant swelling and redness of one digit, 2: mild swelling and erythema of the limb or swelling of more than two digits, 3: marked swelling and erythema of the limb, 4: maximal swelling and redness of the limb and later, ankylosis. The average macroscopic score was expressed as a cumulative value for all paws, with a maximum possible score of 16.

Thioglycollate-induced peritonitis

Mice were injected with 1 ml of 4% sterile thioglycollate intraperitoneally. Four hours later, mice were killed and peritoneal lavage fluid was collected by washing the peritoneal cavity with cold PBS containing 5 mM EDTA and 10 U/ml heparin.

Administration of TFM-C or celecoxib

TFM-C and celecoxib were synthesized as previously described [23]. We injected TFM-C or celecoxib intraperitonealy (i.p.) in 0.5% Tween/5% DMSO/PBS. In CIA experiments, mice received 10 μg/g TFM-C or celecoxib every other day from 21 days after immunuization. In CAIA, we injected the mice with 10 μg/g of TFM-C or celecoxib every other day starting at two days before disease induction. In thioglycollate-induced peritonitis experiments, mice received 10 μg/g of TFM-C or celecoxib two days and one hour before thioglycollate injection. The control animals were injected with vehicle alone.

Histopathology

Arthritic mice were sacrificed and all four paws were fixed in buffered formalin, decalcified, embedded in paraffin, sectioned, and then stained with H&E. Histological assessment of joint inflammation was scored as follows: 0: normal joint, 1: mild arthritis: minimal synovitis without cartilage/bone erosions, 2: moderate arthritis: synovitis and erosions but joint architecture maintained, 3: severe arthritis; synovitis, erosions, and loss of joint integrity. The average of the macroscopic score was expressed as a cumulative value of all paws, with a maximum possible score of 12.

Mast cells in synovium were visually assessed for intact versus degranulating mast cells using morphologic criteria. Mast cells were identified as those cells that contained toluidine blue-positive granules. Only cells in which a nucleus was present were counted. Degranulating cells were defined by the presence of granules outside the cell border with coincident vacant granule space within the cell border as described previously [25].

Measurement of CII specific IgG1 and IgG2a

Bovine CII (1 mg/ml) was coated onto ELISA plates (Sumitomo Bakelite, Co., Ltd, Tokyo, Japan) at 4°C overnight. After blocking with 1% bovine serum albumin in PBS, serially diluted serum samples were added onto CII-coated wells. For detection of anti-CII Abs, the plates were incubated with biotin-labeled anti-IgG1 and anti-IgG2a (Southern Biotechnology Associates, Inc., Brimingham, AL, USA) or anti-IgG Ab (CN/Cappel, Aurora, OH, USA) for one hour and then incubated with streptavidin-peroxidase. After adding a substrate, the reaction was evaluated as OD_{450} values.

Stimulation of or macrophages

B6 mice received 10 μg/g of TFM-C or control vehicle on Day 0 and Day 2, and on Day 3, splenic macrophages were collected and were stimulated by LPS *in vitro* in the presence of TFM-C or vehicle.

Detection of cytokines

Cytokine levels in the culture supernatant were determined by using a sandwich ELISA. The Abs for IL-1β ELISA were purchased from BD Biosciences (San Jose, CA, USA) and the ELISA Abs for IL-6 and TNFα were purchased from eBioscience (San Diego, CA, USA).

Statistical analysis

CIA and CAIA clinical or pathological scores for groups of mice are presented as the mean group clinical score + SEM, and statistical differences were analyzed with a non-parametric Mann-Whitney *U*-test. Data for cytokines were analyzed by an unpaired t-test.

Results

TFM-C inhibits cytokine secretion from activated U937 cells concomitant with induction of an ER stress response

In a recombinant cell system, TFM-C inhibits IL-12 secretion via a mechanism involving the induction of ER stress coupled to intracellular degradation of the cytokine polypeptide chains via the ER stress protein HERP [23,24,26]. In order to verify whether the cytokine secretion-inhibitory effect of TFM-C extends to natural cytokine producer cells, we assessed its effect using PMA/LPS-activated U937 macrophages, a well-known source of multiple cytokines. TFM-C potently blocked secretion of IL-β, IL-6, IL-8, IL-10, IL-12 and TNF-α (Figure 1A, C). By means of QPCR, TFM-C was found to suppress mRNA production of IL-10 over the course of the experiment, and at 12 and 24 h of TFM-C treatment, of IL-1β. Virtually no effect was seen on mRNA production of TNF-α and IL-8, while TFM-C increased IL-6 mRNA between 6 and 12 h. To verify whether TFM-C induced an ER stress response in U937 cells, we measured mRNA of HERP and IL-23p19, both of which have been associated with induction of ER stress [24,26,27]. This showed significant up-regulation of both genes by TFM-C while the housekeeping gene GAPDH was not affected (Figure 1D). Viability of U937 cells following exposure to TFM-C was assessed using two different methods (Figure 1B), and showed a limited percentage of apoptotic cells not exceeding 15 to 20% following 12 to 24 h of treatment. Thus, TFM-C blocks cytokine secretion in natural producer cells by ER stress-related mechanisms that may involve repressive effects on both cytokine mRNA production as well as on post-transcriptional and -translational events involved in cytokine secretion, such as the ER-retention

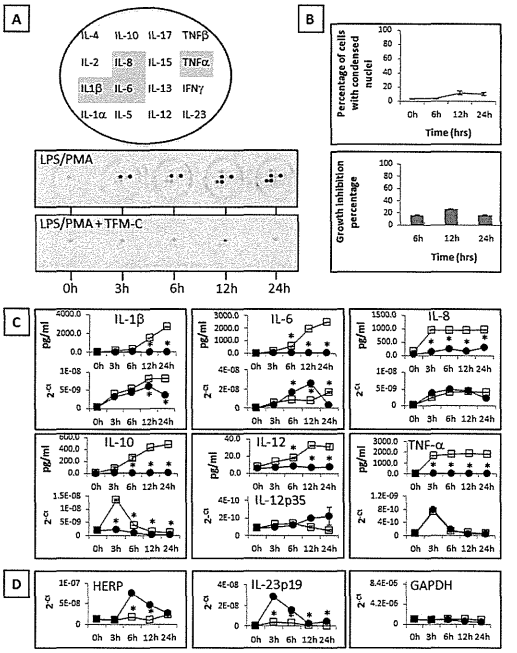

Figure 1 Effect of TFM-C on cytokine production from activated U937 macrophages. A. Lay-out of cytokine-specific antibody spots in the 16-plex cytokine Stripwell array (upper image) and visualization of cytokine-specific chemiluminescence in culture medium of LPS/PMA-treated U937 cells in the absence or presence of TFM-C (lower images). The grey-shaded cytokines in the upper images are those showing the highest production in LPS/PMA-treated U937 cells at 24 h. **B**. Effect of TFM-C treatment (50 μM) on the viability of macrophages (PMA-stimulated U937 cells). Apoptotic cells were measured by DAPI staining, and the percentage of damaged DNA and condensed chromatin was calculated following 6, 12 and 24 h of TFM-C treatment (upper graph). Metabolic activity of cells, measured by AlarmBlue®, was expressed as growth inhibition percentage of untreated controls for 6, 12 and 24 h of TFM-C treatment (lower graph). Bars show average of three independent experiments with corresponding error bars. **C**. Quantification of the kinetics of cytokine secretion and mRNA production (IL-1β, IL-6, IL-8, IL-10 IL-12 and TNF-α) in differentiated macrophages treated with LPS/PMA in the absence (open squares) or presence (solid circles) of TFM-C. All values represent the averages of three independent experiments. For each cytokine, the upper graph represents amount of secreted cytokine quantified using Quansys 16-plex Stripwells, while the lower graph represents cytokine-specific mRNA quantified by QPCR. Asterisks indicate significant differences at * $P < 0.05$ between TFM-C-treated and -untreated cells at each time point using Student's *t*-test. **D**. Effect of 50 μM TFM-C on IL-23p19, HERP and GAPDH mRNAs (QPCR) in differentiated macrophages, stimulated by LPS and PMA. The levels of mRNA levels are shown as 2^{-Ct}. Asterisks indicate significant differences at * $P < 0.05$ compared with baseline condition LPS/PMA-only using Student's *t*-test.

coupled to HERP-mediated degradation identified before for IL-12 [23,24,26]. However, of the TFM-C-sensitive cytokines identified in this experiment, IL-1β follows an unconventional protein secretion route involving

exocytosis of endolysosome-related vesicles not derived from the ER/Golgi system [28]. Given its blockage by TFM-C, which can not be explained by partial suppression of mRNA levels only, this indicates that TFM-C may suppress secretion of cytokines via interfering with both conventional ER-dependent and unconventional ER-independent transit routes.

TFM-C inhibits CIA

First, we examined the effect of TFM-C on CIA induced by immunizing DBA1/J mice with type II collagen. As shown in Figure 2A, administration of TFM-C strongly suppressed the severity of arthritis compared with vehicle-treated mice (*P*-value, < 0.05 by Mann-Whitney *U*-test compared with control from Day 26 and Day 36.). In contrast, administration of celecoxib showed only a mild suppressive effect on CIA, which is consistent with a previous report [19] (*P*-value, < 0.05 by Mann-Whitney *U*-test compared with control at Day 29 and Day 31.) In addition to visual scoring, we analyzed the histological features in the joints of four paws from TFM-C-, celecoxib- or vehicle-treated mice 37 days after disease induction. Quantification of the histological severity of arthritis is shown in Figure 2B and typical histological features are demonstrated in Figure 2C. Arthritis was not apparent in joints treated with TFM-C (Figure 2C, rightmost panel) compared to the severe arthritis with massive cell infiltration, cartilage erosion and bone destruction seen in joints of animals treated with vehicle (Figure 2C, leftmost panel). Both the clinical scores and pathological features of arthritis were significantly less severe in TFM-C-treated mice (Figure 2A-C). The pathological features, including cell infiltration and destruction of cartilage and bone, were slightly less severe in celecoxib-treated mice even though there is no statistically significant difference compared to vehicle-treated mice (Figure 2B). We next examined anti-CII antibody in TFM-C-, celecoxib- or vehicle-treated arthritic mice. There was a trend for reduction in both IgG1 and IgG2a isotypes as well as total IgG anti-CII in TFM-C-treated mice compared to vehicle-treated mice (Figure 2D), but the difference did not reach statistical significance. These results indicate that TFM-C possesses a potent inhibitory effect on CIA compared to vehicle or celecoxib. However, TFM-C treatment had little effect on CII-specific responses.

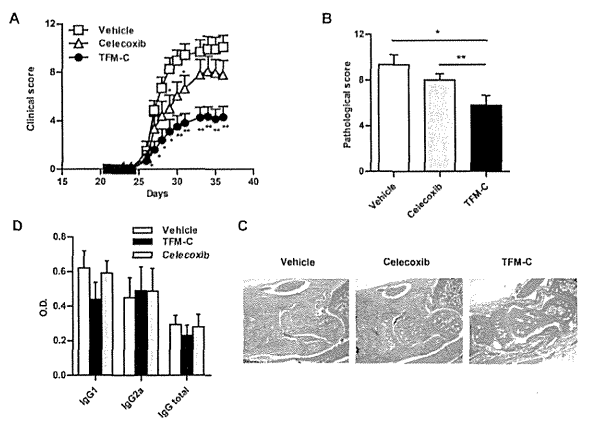

Figure 2 The effect of TFM-C on CIA. A. Clinical scores of CIA in DBA1/J mice treated with 10 μg/g TFM-C (closed circles), celecoxib (open triangles) or vehicle (open squares) every other day from 21 days after immunization. The data shown are pooled from two similar experiments. Error bars represent + SEM of 10 to 12 mice per group. * $P < 0.05$ compared with control group. * $P < 0.05$ compared with both control and celecoxib-treated groups. **B**. Quantification of histological assessment of joints 37 days after induction of CIA. Result shown is the mean + SEM of five mice per group. * $P < 0.05$, TFM-C-treated versus vehicle-treated group. * $P < 0.05$, celecoxib-treated versus TFM-C-treated group. **C**. Representative histological feature of joints in vehicle-treated (left), TFM-C-treated (right) and celecoxib-treated (middle) mice. (H&E stained; original magnification × 40). **D**. The effect of TFM-C on CII-specific response. CII-specific antibody responses in vehicle- (open bars), TFM-C- (filled bars) and celecoxib-treated (gray bars) group. Individual serum samples were obtained at Day 37 after the induction of arthritis and were analyzed as indicated in Materials and Methods. Data represent the mean + SEM of five mice per group.

TFM-C inhibits CAIA

Although TFM-C treatment suppressed clinical and pathological severities of CIA, CII-specific antibody levels were not reduced by TFM-C treatment. Therefore, we hypothesized that TFM-C treatment may have a strong inhibitory effect on the effector phase of arthritis. To test this hypothesis, we examined the effect of TFM-C on CAIA induced by injecting a mixture of monoclonal antibodies against type II collagen (CII) followed by lipopolysaccharide (LPS) administration two days later. The major players in CAIA are innate immune cells while adaptive immune cells are not required for disease development. Therefore, CAIA has value as an animal model to study the effector phase of arthritis. In vehicle-treated mice, severe arthritis occurred one week after CII antibody injection, and administration of celecoxib inhibited arthritis slightly (Figure 3A). In contrast, administration of TFM-C significantly suppressed CAIA compared to vehicle or celecoxib treatment. We next analyzed the histological features in the joints of four paws from vehicle-, TFM-C- and celecoxib-treated mice 12 days after disease induction. Quantification of the histological severity of arthritis is shown in Figure 3B and typical histological features are presented in Figure 3C. Massive cell infiltration, cartilage erosion, and bone destruction were observed in joints of vehicle-treated or celecoxib-treated mice but not in those of TFM-C-treated mice (Figure

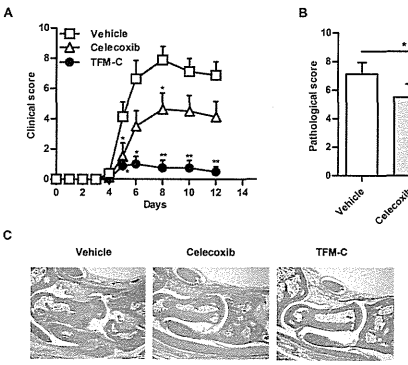

Figure 3 The effect of TFM-C on CAIA. A. Clinical scores of CAIA in B6 mice treated with 10 μg/g TFM-C (closed circles), celecoxib (open triangles) or vehicle (open squares) every other day from two days before CAIA induction. * $P < 0.05$ compared with control group, * $P < 0.05$ compared with both control and celecoxib-treated groups. Results shown are the mean + SEM of five mice per group. The data shown are from a single experiment representative of two similar experiments. **B.** Quantification of histological assessment of joints 12 days after induction of AIA shown in A. Results shown are the mean + SEM of five mice per group. * $P < 0.05$ control versus TFM-C group, * $P < 0.05$ celecoxib versus TFM-C -treated group. **C.** Representative histological feature of joints in vehicle-treated (left), TFM-C-treated (middle) and celecoxib-treated (right) mice. (H&E stained; original magnification × 40).

3B, C). These results indicate that TFM-C exhibits a strong disease inhibitory effect in CAIA in contrast to vehicle or celecoxib.

TFM-C inhibits the mast cell activation in CAIA

Next, we sought to understand the mechanism through which TFM-C treatment suppressed arthritis in CAIA. Since mast cells have been demonstrated to be critical for initiation of antibody-induced arthritis [29], we evaluated the effect of TFM-C on the activation of mast cells. Because degranulation is the clearest histological hallmark of mast cell activation, joint mast cells were visually assessed for an intact versus degranulating phenotype after staining with toluidine blue. The proportion of degranulated mast cells was significantly lower in TFM-C-treated mice compared to that in celecoxib- or vehicle-treated mice (Figure 4A, B).

TFM-C supresses the activation of macrophages

Innate immune cells and inflammatory cytokines, such as IL-1 and TNF-α are critical for disease development in CAIA [30]. Thus, we next determined the effect of TFM-C on the production of inflammatory cytokines from macrophages. Splenic macrophages from mice treated with TFM-C, celecoxib or control vehicle, were stimulated with LPS *ex vivo*, and the cytokines in the culture supernatants were measured by ELISA. The production of IL-1, IL-6 and TNF-α from macrophages was efficiently suppressed in TFM-C-treated mice compared to vehicle-treated mice (Figure 5). In celecoxib-treated mice, although the production of IL-1β was decreased, the production of other cytokines such as IL-6 and TNF-α was not suppressed, and the IL-6 production was even enhanced compared to vehicle-treated mice.

TFM-C suppresses leukocyte influx in thioglycollate-induced peritonitis

The other key players in antibody-induced arthritis are neutrophils [31-34]. Neutrophils are recruited to joint tissue and depletion of neutrophils has been shown to supress disease susceptibility and severity in CAIA [35]. An intraperitoneal injection of thioglycollate causes leukocytes influx into the peritoneum from bone marrow and circulation, and neutrophils are the major cell population which first emigrate to the peritoneal cavity. To assess the effect of TFM-C on neutrophil recruitment, mice were treated with TFM-C, celecoxib or control vehicle, and thioglycollate was injected intraperitoneally. Leukocyte cell numbers in the peritoneal cavity four hours after thioglycollate injection were comparable between control and celecoxib-treated groups (Figure 6). However, the peritoneal infiltrating cell numbers were reduced in mice treated with TFM-C, suggesting the suppressive effect of TFM-C on neutrophil recruitment.

Taken together, these results indicate that the activation of innate immune cells, including mast cells, macrophages, and neutrophils, is suppressed in TFM-C-treated mice but not in celecoxib-treated mice.

Discussion

In the present study we demonstrate, using arthritis models, that TFM-C, a celecoxib analogue with 205-fold lower COX-2-inhibitory activity, inhibits autoimmune disease. TFM-C differs from celecoxib by the substitution of the 4-methyl group by a trifluoromethyl group. This substitution drastically increases the IC_{50}s for inhibition of COX1 (15 μM to >100 μM for celecoxib and TFM-C, respectively) and COX2 (0.04 μM to 8.2 μM, respectively), but does not affect the apoptotic index measured in PC3 prostate cancer cells, indicating independence between structural requirements for COX-2 inhibition and apoptosis induction [36]. Celecoxib perturbs intracellular calcium by blocking ER Ca^{2+} ATPases, and this activity is shared with TFM-C [23,37]. In a HEK293 recombinant cell system, this Ca^{2+} perturbation is associated with inhibition of secretion and altered intracellular interaction of IL-12 polypeptide chains with the ER chaperones calreticulin and ERp44, and results in the interception of IL-12 by HERP

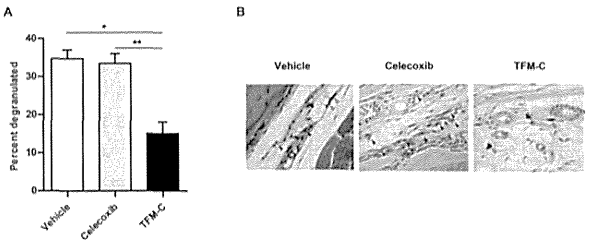

Figure 4 TFM-C inhibits the mast cell activation in CAIA. CAIA was induced in B6 mice and the mice were then treated with 10 μg/g TFM-C, celecoxib or vehicle as described in Figure 2. **A.** Quantification of degranulated mast cells in synovium of joints 12 days after induction of CAIA. * $P < 0.05$, compared with vehicle-treated group. * $P < 0.05$, compared with celecoxib-treated group. Results shown are the mean + SEM of six mice per group and were pooled from two experiments. **B.** Hisopathologic features of degranulated or intact mast cells in joints of representative vehicle-, celecoxib- and TFM-C- treated mice (toluidine blue stained; original magnification, × 100). White arrows indicate intact mast cells and black arrows indicate degranulated mast cells.

followed by degradation of the cytokine [23,24,26]. While IC_{50}s for inhibition of IL-12 secretion by celecoxib or TFM-C are similar [23,24], in the present paper, we show that TFM-C inhibits production of various cytokines from activated macrophages (Figures 1 and 5) and exerts a strikingly stronger inhibitory effect on arthritis models compared to celecoxib. Given that the main biological difference between celecoxib and TFM-C resides in the extent of COX-1 and -2 inhibition, it is, therefore, likely that the less potent effect of TFM-C on COX1/2 inactivation is a contributing, disease-limiting rather than disease-promoting factor in these arthritis models. Indications supporting this concept come from a study showing increased LPS-induced macrophage production of TNF-α by inactivation of COX-2 with celecoxib [38]. Up-regulation of TNF-α by celecoxib was also reported in human PBMCs, rheumatoid synovial cultures and whole blood [20]. The relation between the anticipated extent of COX inhibition and production of TNF-α was observed in the present study (Figure 5), where activated macrophages showed a tendency toward increased or decreased TNF-α production in the presence of celecoxib or TFM-C, respectively, compared to vehicle-treated cells. In this cell system (Figure 5), celecoxib significantly increased production of the pro-inflammatory cytokine IL-6 while TFM-C suppressed it. Pending future mechanistic studies, this data indicate that prostaglandin-mediated suppressive effects, or other, as yet to be identified differential TFM-C/celecoxib-related effects on TNF-α production may extend to other cytokines as well, and provide an important clue as to the more potent beneficial effects of TFM-C compared to celecoxib in the arthritis models presented here.

The suppression of antibody-induced arthritis, which requires innate but not acquired immune cells [29-34,39], suggests that TFM-C also inhibits the activation of innate immune cells while celecoxib does not. In fact, TFM-C suppresses the production of inflammatory cytokines from macrophages and the activation of mast cells as well as the subsequent recruitment of leukocytes. Mast cells are essential for the initiation of antibody-induced arthritis [29]. Moreover, mast cells are present in human synovia [40-43] and are an important

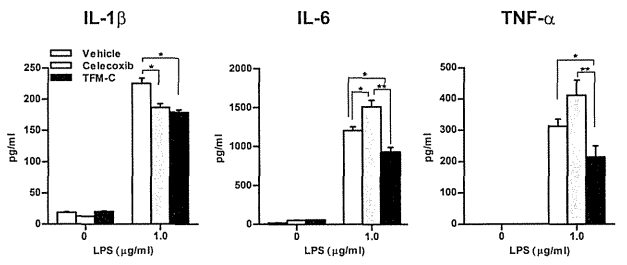

Figure 5 TFM-C supresses the activation of macrophages. B6 mice recieved 10 μg/g TFM-C, celecoxib or vehicle on Day 0 and Day 2, and on Day 3, splenic macrophages were collected and were stimulated by LPS *in vitro* in the presence of TFM-C, celecoxib or vehicle. Cytokines were detected by ELISA. IL-1β and IL-6 were measured 24 h after stimulation. TNF-α was measured six hours after stimulation. The data shown are from a single experiment representative of three similar experiments. * $P < 0.05$ compared with control group, * $P < 0.05$ compared with celecoxib-treated group.

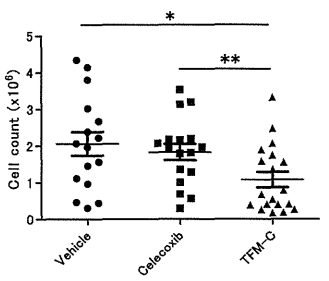

Figure 6 TFM-C supresses leukocyte influx in thioglycollate-induced peritonitis. B6 mice recieved 10 μg/g TFM-C, celecoxib or vehicle at two days and one hour before peritoneal injection of thioglycollate. At four hours after thioglycollate injection, peritoneal lavage fluid was collected and the infiltrating cells were counted. Cell numbers are shown from three separate experiments. * $P <$ 0.05, TFM-C-treated versus vehicle-treated group. * $P < 0.05$, celecoxib-treated versus TFM-C-treated group.

source of both proteases and inflammatory cytokines, including IL-17, in patients with rheumatoid arthritis [42-44]. The clear difference between the effects of TFM-C and celecoxib on the suppression of mast cell activation could explain the differential impact of these compounds on arthritis models. Mast cells are important not only in arthritis but also in other conditions, such as allergy, obesity and diabetes [45]. Therefore, the suppression of mast cell activation by TFM-C may be applicable for the inhibition of these diseases in addition to autoimmune diseases.

Cytokines and chemokines, such as TNF-α and MCP-1, produced by macrophages, are suggested to play important roles for neutrophil influx in thioglycollate-induced peritonitis [46]. Mast cells were shown to produce TNF-α, which recruits neutrophils into the peritoneum in an immune complex peritonitis model [47]. Thus, it is likely that TFM-C suppressed macrophages and mast cells produce such chemoattractants, which in turn inhibited neutrophil influx into the peritoneum. However, it is also possible that TFM-C directly suppressed neutrophil activation. Further studies are required to address this possibility.

As described above, the major players in CAIA are innate immune cells, while adaptive immune cells are not required for disease development. Therefore, CAIA has value as an animal model for the study of the effector phase of arthritis. However, it is well known that adaptive immune cells play a significant role in the pathogenesis of RA and the strongest genetic link in RA is the association with HLA-DR, which is thought to present autoantigens to T cells. The activation of T cells and B cells is believed to initiate and/or enhance the effector inflammation phase of arthritis. In fact, massive infiltration of T and B cells is observed in RA synovium. Therefore, the ideal therapeutic agents for RA are those displaying the capacity to suppress both the induction and effector phases of arthritis. TFM-C treatment suppresses CIA, which requires both innate and adaptive immune cells for the development of arthritis. We previously demonstrated that celecoxib treatment suppresses EAE induced by immunizing B6 mice with myelin oligodendrocyte glycoprotein$_{35-55}$ (MOG) peptide [22]. The suppression of EAE by celecoxib was COX-2 independent and was accompanied by reduced IFN-γ production by MOG-reactive T cells. We observed a trend of reduced anti-CII antibody levels in serum upon TFM-C treatment. As TFM-C inhibited secretion of both recombinant IL-12 and IL-23 using a pIND ponasterone-inducible vector system in HEK293 cells [23,24], TFM-C treatment may have also influenced CII-specific immune responses by suppressing antigen-presenting cells.

Specific inhibition of COX-2 has some adverse effects. Rofecoxib, a highly specific COX-2 inhibitor, was withdrawn from the world market because of an increased rate of cardiovascular events in patients with colorectal polyps [48]. Celecoxib was also shown to augment cardiovascular and thrombotic risk in colorectal adenoma patients, especially in the subgroup suffering from pre-existing atherosclerotic heart disease [49]. Moreover, inhibition of COX-2 activity has been reported to exacerbate brain inflammation by increasing glial cell activation [50]. It has been suggested that the inhibition of COX-2-dependent prostaglandin I_2 from endothelial cells may be the major cause of thrombosis [51]. As the COX-2-inhibitory activity of TFM-C is 205-fold lower than that of celecoxib, the arthritis suppression by TFM-C appears to be independent of COX-2 inhibition. Therefore, TFM-C, which has strong immunoregulatory abilities but low COX-2-inhibitory activity, could serve as a new disease-modifying agent to prevent the progression of autoimmune diseases such as RA.

Conclusions

In summary, TFM-C, a trifluoromethyl analogue of celecoxib, inhibits arthritis despite the fact that TFM-C possesses very low COX-2-inhibitory activity. The most striking features of TFM-C are its inhibitory effect on the activation of innate immune cells and its suppression of arthritis compared to celecoxib. TFM-C treatment suppressed both CIA and CAIA by targeting innate immune cells, which are involved in both the induction and the effector phases of arthritis inflammation. Taking these data together, TFM-C may serve as an effective therapeutic drug for arthritis, including RA.

Abbreviations

B6: C57BL/6J; CII: anti-type II collagen; CAIA: type II collagen antibody-induced arthritis; CFA: complete Freund's adjuvant; CIA: collagen-induced arthritis; COX-2: cycolooxygenase-2; EAE: experimental autoimmune

encephalomyelitis; ELISA: enzyme-linked immunosorbent assay; IFA: incomplete Freund's adjuvant; IL: interleukin; LPS: lipopolysaccharide; MOG: myelin oligodendrocyte glycoprotein; *Mtb*: *Mycobacterium tuberculosis*; PBS: phosphate-buffered saline; TFM-C: a trifluoromethyl analogue of celecoxib; TNF: tumor necrosis factor.

Acknowledgements
This work was supported by Japan Foundation for Neuroscience and Mental Health (AC), a Grant-in-Aid for Scientific Research (B: 7210 to SM) from the Japan Society for the Promotion of Science, and Health and Labour Sciences Research Grants on Intractable Diseases (Neuroimmunological Diseases) from the Minitry of Health, Labour and Welfare of Japan; and by grants to KV from the Ministerio de Ciencia e Innovación, Madrid, Spain (MEC-2008; SAF2008-00433) and from the Gobierno Vasco's SAIOTEK Program (Ref. S-PE09UN33).

Author details
[1]Department of Immunology, National Institute of Neuroscience, National Center of Neurology and Psychiatry, 4-1-1 Ogawahigashi, Kodaira, Tokyo 187-8502, Japan. [2]Neurogenomiks Laboratory, Universidad Del País Vasco (UPV/EHU), Parque Tecnológico de Bizkaia, 48170 Zamudio, Spain. [3]IKERBASQUE, Basque Foundation for Science, 48011, Bilbao, Spain.

Authors' contributions
AC, MM, CT, RT and AP performed and evaluated experiments. AC, TY, KV and SM designed and supervised the experiments. IA and KV provided TFM-C. AC, KV and SM prepared the manuscript. All authors have read and approved the manuscript for publication.

Competing interests
The authors declare that they have no competing interests.

Received: 14 June 2011 Revised: 13 December 2011
Accepted: 17 January 2012 Published: 17 January 2012

References

1. Krieckaert CL, Bartelds GM, Lems WF, Wolbink GJ: **The effect of immunomodulators on the immunogenicity of TNF-blocking therapeutic monoclonal antibodies: a review.** *Arthritis Res Ther* 2010, **12**:217.
2. Feldmann M, Maini SR: **Role of cytokines in rheumatoid arthritis: an education in pathophysiology and therapeutics.** *Immunol Rev* 2008, **223**:7-19.
3. Buch MH: **Sequential use of biologic therapy in rheumatoid arthritis.** *Curr Opin Rheumatol* 2010, **22**:321-329.
4. Nishimoto N, Yoshizaki K, Miyasaka N, Yamamoto K, Kawai S, Takeuchi T, Hashimoto J, Azuma J, Kishimoto T: **Treatment of rheumatoid arthritis with humanized anti-interleukin-6 receptor antibody: a multicenter, double-blind, placebo-controlled trial.** *Arthritis Rheum* 2004, **50**:1761-1769.
5. Maini RN, Taylor PC, Szechinski J, Pavelka K, Bröll J, Balint G, Emery P, Raemen F, Petersen J, Smolen J, Thomson D, Kishimoto T, CHARISMA Study Group: **Double-blind randomized controlled clinical trial of the interleukin-6 receptor antagonist, tocilizumab, in European patients with rheumatoid arthritis who had an incomplete response to methotrexate.** *Arthritis Rheum* 2006, **54**:2817-2829.
6. Genovese MC, McKay JD, Nasonov EL, Mysler EF, da Silva NA, Alecock E, Woodworth T, Gomez-Reino JJ: **Interleukin-6 receptor inhibition with tocilizumab reduces disease activity in rheumatoid arthritis with inadequate response to disease-modifying antirheumatic drugs: the tocilizumab in combination with traditional disease-modifying antirheumatic drug therapy study.** *Arthritis Rheum* 2008, **58**:2968-2980.
7. Smolen JS, Beaulieu A, Rubbert-Roth A, Ramos-Remus C, Rovensky J, Alecock E, Woodworth T, Alten R, OPTION Investigators: **Effect of interleukin-6 receptor inhibition with tocilizumab in patients with rheumatoid arthritis (OPTION study): a double-blind, placebo-controlled, randomized trial.** *Lancet* 2008, **371**:987-997.
8. Emery P, Fleischmann R, Filipowicz-Sosnowska A, Schechtman J, Szczepanski L, Kavanaugh A, Racewicz AJ, van Vollenhoven RF, Li NF, Agarwal S, Hessey EW, Shaw TM, DANCER Study Group: **The efficacy and safety of rituximab in patients with active rheumatoid arthritis despite methotrexate treatment: results of a phase IIB randomized, double-blind, placebo-controlled, dose-ranging trial.** *Arthritis Rheum* 2006, **54**:1390-1400.
9. Cohen SB, Emery P, Greenwald MW, Dougados M, Furie RA, Genovese MC, Keystone EC, Loveless JE, Burmester GR, Cravets MW, Hessey EW, Shaw T, Totoritis MC, REFLEX Trial Group: **Rituximab for rheumatoid arthritis refractory to anti-tumor necrosis factor therapy: results of a multicenter, randomized, double-blind, placebo-controlled, phase III trial evaluating primary efficacy and safety at twenty-four weeks.** *Arthritis Rheum* 2006, **54**:2793-2806.
10. Kremer JM, Westhovens R, Leon M, Di Giorgio E, Alten R, Steinfeld S, Russell A, Dougados M, Emery P, Nuamah IF, Williams GR, Becker JC, Hagerty DT, Moreland LW: **Treatment of rheumatoid arthritis by selective inhibition of T-cell activation with fusion protein CTLA4Ig.** *N Engl J Med* 2003, **349**:1907-1915.
11. Lopez-Diego RS, Weiner HL: **Novel therapeutic strategies for multiple sclerosis-a multifaceted adversary.** *Nat Rev Drug Discov* 2008, **7**:909-925.
12. Yazici Y: **Treatment of rheumatoid arthritis: we are getting there.** *Lancet* 2009, **374**:178-180.
13. Myers LK, Kang AH, Postlethwaite AE, Rosloniec EF, Morham SG, Shlopov BV, Goorha S, Ballou LR: **The genetic ablation of cyclooxygenase 2 prevents the development of autoimmune arthritis.** *Arthritis Rheum* 2000, **43**:2687-2693.
14. Trebino CE, Stock JL, Gibbons CP, Naiman BM, Wachtmann TS, Umland JP, Pandher K, Lapointe JM, Saha S, Roach ML, Carter D, Thomas NA, Durtschi BA, McNeish JD, Hambor JE, Jakobsson PJ, Carty TJ, Perez JR, Audoly LP: **Impaired inflammatory and pain responses in mice lacking an inducible prostaglandin E synthase.** *Proc Natl Acad Sci USA* 2003, **100**:9044-9049.
15. Honda T, Segi-Nishida E, Miyachi Y, Narumiya S: **Prostacyclin-IP signaling and prostaglandin E2-EP2/EP4 signaling both mediate joint inflammation in mouse collagen-induced arthritis.** *J Exp Med* 2006, **203**:325-335.
16. Noguchi M, Kimoto A, Kobayashi S, Yoshino T, Miyata K, Sasamata M: **Effect of celecoxib, a cyclooxygenase-2 inhibitor, on the pathophysiology of adjuvant arthritis in rat.** *Eur J Pharmacol* 2005, **513**:229-235.
17. Tsuboi H, Nampei A, Matsui Y, Hashimoto J, Kawai S, Ochi T, Yoshikawa H: **Celecoxib prevents juxta-articular osteopenia and growth plate destruction adjacent to inflamed joints in rats with collagen-induced arthritis.** *Mod Rheumatol* 2007, **17**:115-122.
18. Taketa T, Sakai A, Tanaka S, Nakai K, Menuki K, Yamane H, Tanaka K, Nakamura T: **Selective cyclooxygenase-2 inhibitor prevents reduction of trabecular b:one mass in collagen-induced arthritic mice in association with suppression of RANKL/OPG ratio and IL-6 mRNA expression in synovial tissues but not in bone marrow cells.** *J Bone Miner Metab* 2008, **26**:143-151.
19. Anderson GD, Keys KL, De Ciechi PA, Masferrer JL: **Combination therapies that inhibit cyclooxygenase-2 and leukotriene synthesis prevent disease in murine collagen induced arthritis.** *Inflamm Res* 2009, **58**:109-117.
20. Page TH, Turner JJ, Brown AC, Timms EM, Inglis JJ, Brennan FM, Foxwell BM, Ray KP, Feldmann M: **Nonsteroidal anti-inflammatory drugs increase TNF production in rheumatoid synovial membrane cultures and whole blood.** *J Immunol* 2010, **185**:3694-3701.
21. Grosch S, Tegeder I, Niederberger E, Brautigam L, Geisslinger G: **COX-2 independent induction of cell cycle arrest and apoptosis in colon cancer cells by the selective COX-2 inhibitor celecoxib.** *FASEB J* 2001, **15**:2742-2744.
22. Miyamoto K, Miyake S, Mizuno M, Oka N, Kusunoki S, Yamamura T: **Selective COX-2-inhibitor celecoxib prevents experimental autoimmune encephalomyelitis through COX-2-independent pathway.** *Brain* 2006, **129**:1984-1992.
23. Alloza I, Baxter A, Chen Q, Matthiesen R, Vandenbroeck K: **Celecoxib inhibits interleukin-12 alphabeta and beta2 folding and secretion by a novel COX2-independent mechanism involving chaperones of the endoplasmic reticulum.** *Mol Pharmacol* 2006, **69**:1579-1587.
24. McLaughlin M, Alloza I, Quoc HP, Scott CJ, Hirabayashi Y, Vandenbroeck K: **Inhibition of secretion of interleukin (IL)-12/23 family cytokines by 4-trifluoromethyl-celecoxib is coupled to degradation via the endoplasmic reticulum stress protein HERP.** *J Biol Chem* 2010, **285**:6960-6969.
25. Kaieda S, Tomi C, Oki S, Yamamura T, Miyake S: **Activation of invariant natural killer T cells by synthetic glycolipid ligands suppresses autoantigody-induced arthritis.** *Arthritis Rheum* 2007, **56**:1836-1845.

26. McLaughlin M, Vandenbroeck K: **The endoplasmic reticulum protein folding factory and its chaperones: new targets for drug discovery?** *Br J Pharmacol* 2011, **162**:328-345.
27. Wheeler MC, Rizzi M, Sasik R, Almanza G, Hardiman G, Zanetti M: **KDEL-retained antigen in B lymphocytes induces a proinflammatory response: a posible role for endoplasmic reticulum stress in adaptive T cell immunity.** *J Immunol* 2008, **181**:256-264.
28. Andrei C, Dazzi C, Lotti L, Torrisi MR, Chimini G, Rubartelli A: **The secretory route of the leaderless protein interleukin 1beta involves exocytosis of endolysosome-related vesicles.** *Mol Biol Cell* 1999, **10**:1463-1475.
29. Lee DM, Friend DS, Gurish MF, Benoist C, Mathis D, Brenner MB: **Mast cells: a cellular link between autoantibodies and inflammatory arthritis.** *Science* 2002, **297**:1689-1692.
30. Kagari T, Doi H, Shimozato T: **The importance of IL-1 beta and TNF-alpha, and the noninvolvement of IL-6, in the development of monoclonal antibody-induced arthritis.** *J Immunol* 2002, **169**:1459-1466.
31. Chen M, Lam BK, Kanaoka Y, Nigrovic PA, Audoly LP, Austen KF, Lee DM: **Neutrophil-derived leukotriene B4 is required for inflammatory arthritis.** *J Exp Med* 2006, **203**:837-842.
32. Kim ND, Chou RC, Seung E, Tager AM, Luster AD: **A unique requirement for the leukotriene B4 receptor BLT1 for neutrophil recruitment in inflammatory arthritis.** *J Exp Med* 2006, **203**:829-835.
33. Zhou JS, Xing W, Friend DS, Austen KF, Katz HR: **Mast cell deficiency in Kit (W-sh) mice does not impair antibody-mediated arthritis.** *J Exp Med* 2007, **204**:2797-802.
34. Chou RC, Kim ND, Sadik CD, Seung E, Lan Y, Byme MH, Haribabu B, Iwakura Y, Luster AD: **Lipid-cytokine-chemokine cascade drives neutrophil recruitment in a murine model of inflammatory arthritis.** *Immunity* 2010, **33**:266-278.
35. Nandakumar KS, Svensson L, Holmdahl R: **Collagen type II-specific monoclonal antibody-induced arthritis in mice: description of the disease and the influence of age, sex, and genes.** *Am J Pathol* 2003, **163**:1827-1837.
36. Zhu J, Song X, Lin HP, Young DC, Yan S, Marquez VE, Chen CS: **Using cyclooxygenase-2 inhibitors as molecular platforms to develop a new class of apoptosis-inducing agents.** *J Natl Cancer Inst* 2002, **94**:1745-1757.
37. Johnson AJ, Hsu AL, Lin HP, Song X, Chen CS: **The cyclo-oxygenase-2 inhibitor celecoxib perturbs intracellular calcium by inhibiting endoplasmic reticulum Ca2+-ATPases: a plausible link with its anti-tumour effect and cardiovascular risks.** *Biochem J* 2002, **366**:831-837.
38. Gitlin JM, Loftin CD: **Cyclooxygenase-2 inhibition increases lipopolysaccharide-induced atherosclerosis in mice.** *Cardiovasc Res* 2009, **81**:400-407.
39. Wipke BT, Allen PM: **Essential role of neutrophils in the initiation and progression of a murine model of rheumatoid arthritis.** *J Immunol* 2010, **167**:1601-1608.
40. Bromley M, Fisher WD, Woolley DE: **Mast cells at sites of cartilage erosion in the rheumatoid joint.** *Ann Rheum Dis* 1984, **43**:76-79.
41. Kiener HP, Baghestanian M, Dominkus M, Walchshofer S, Ghannadan M, Willheim M, Sillaber C, Graninger WB, Smolen JS, Valent P: **Expression of the C5a receptor (CD88) on synovial mast cells in patients with rheumatoid arthritis.** *Arthritis Rheum* 1998, **41**:233-245.
42. Sawamukai N, Yukawa S, Saito K, Nakayamada S, Kambayashi T, Tanaka Y: **Mast cell-derived tryptase inhibits apoptosis of human rheumatoid synovial fibroblasts via rho-mediated signaling.** *Arthritis Rheum* 2010, **62**:952-959.
43. Eklund KK: **Mast cells in the pathogenesis of rheumatic diseases and as potential targets for anti-rheumatic therapy.** *Immunol Rev* 2007, **217**:38-52.
44. Hueber AJ, Asquith DL, Miller AM, Reilly J, Kerr S, Leipe J, Melendez AJ, McInnes IB: **Mast cells express IL-17A in rheumatoid arthritis synovium.** *J Immunol* 2010, **184**:3336-3340.
45. Liu J, Divoux A, Sun J, Zhang J, Clement K, Glickman JN, Sukhova GK, Wolters PJ, Du J, Gorgun CZ, Doria A, Libby P, Blumberg RS, Kahn BB, Hotamisligil GS, Shi GP: **Genetic deficiency and pharmacological stabilization of mast cells reduce diet-induced obesity and diabetes in mice.** *Nat Med* 2009, **15**:940-945.
46. Matsukawa A, Kudo S, Maeda T, Numata K, Watanabe H, Takeda K, Akira S, Ito T: **Stat3 in resident macrophages are a repressor protein of inflammatory response.** *J Immunol* 2005, **175**:3354-3359.
47. Zhang Y, Ramos BF, Jakschik BA: **Neutrophil recruitment by tumor necrosis factor from mast cells in immune complex peritonitis.** *Science 192* **258**:1957-1959.
48. Bresalier RS, Sandler RS, Quan H, Bolognese JA, Oxenius B, Horgan K, Lines C, Riddell R, Morton D, Lanas A, Konstam MA, Baron JA: **Adenomatous Polyp Prevention on Vioxx (APPROVe) Trial Investigators. Cardiovascular events associated with rofecoxib in a colorectal adenoma chemoprevention trial.** *N Eng J Med* 2005, **352**:1092-1102.
49. Bertagnolli MM, Eagle CJ, Zauber AG, Redston M, Breazna A, Kim K, Tang J, Rosenstein RB, Umar A, Bagheri D, Collins NT, Burn J, Chung DC, Dewar T, Foley TR, Hoffman N, Macrae F, Pruitt RE, Saltzman JR, Salzberg B, Sylwestrowicz T, Hawk ET, Adenoma Prevention with Celecoxib Study Investigators: **Five-year efficacy and safety analysis of the adenoma prevention with celecoxib trial.** *Cancer Prev Res (Phila)* 2009, **2**:310-321.
50. Aid S, Langenbach R, Bosetti F: **Neuroinflammatory response to lipopolysaccharide is exacerbated in mice genetically deficient in cyclooxygenase-2.** *J Neuroinflammation* 2008, **5**:17-30.
51. Kobayashi T, Tahara Y, Matsumoto M, Iguchi M, Sano H, Murayama T, Arai H, Oida H, Yurugi-Kobayashi T, Yamashita JK, Katagiri H, Majima M, Yokode M, Kita T, Narumiya S: **Roles of thromboxane A(2) and prostacyclin in the development of atherosclerosis in apoE-deficient mice.** *J Clin Invest* 2004, **114**:784-794.

doi:10.1186/ar3683
Cite this article as: Chiba *et al.*: A 4-trifluoromethyl analogue of celecoxib inhibits arthritis by suppressing innate immune cell activation. *Arthritis Research & Therapy* 2012 **14**:R9.

ARTHRITIS & RHEUMATISM
Vol. 64, No. 1, January 2012, pp 153–161
DOI 10.1002/art.33314

Mucosal-Associated Invariant T Cells Promote Inflammation and Exacerbate Disease in Murine Models of Arthritis

Asako Chiba, Ryohsuke Tajima, Chiharu Tomi, Yusei Miyazaki, Takashi Yamamura, and Sachiko Miyake

Objective. **The function of mucosal-associated invariant T (MAIT) cells remains largely unknown. We previously reported an immunoregulatory role of MAIT cells in an animal model of multiple sclerosis. The aim of this study was to use animal models to determine whether MAIT cells are involved in the pathogenesis of arthritis.**

Methods. **$MR1^{-/-}$ and $MR1^{+/+}$ DBA/1J mice were immunized with bovine type II collagen (CII) in complete Freund's adjuvant to trigger collagen-induced arthritis (CIA). To assess CII-specific T cell recall responses, lymph node cells from mice with CIA were challenged with CII ex vivo, and cytokine production and proliferation were evaluated. Serum levels of CII-specific antibodies were measured by enzyme-linked immunosorbent assay. Collagen antibody–induced arthritis (CAIA) was induced in $MR1^{-/-}$ and $MR1^{+/+}$ C57BL/6 mice by injection of anti-CII antibodies followed by injection of lipopolysaccharide. To demonstrate the involvement of MAIT cells in arthritis, we induced CAIA in $MR1^{-/-}$ C57BL/6 mice that had been reconstituted with adoptively transferred MAIT cells. MAIT cell activation in response to cytokine stimulation was investigated.**

Results. **The severity of CIA was reduced in $MR1^{-/-}$ DBA/1J mice. However, T and B cell responses to CII were comparable in $MR1^{-/-}$ and $MR1^{+/+}$ DBA/1J mice. $MR1^{-/-}$ C57BL/6 mice were less susceptible to CAIA, and reconstitution with MAIT cells induced severe arthritis in $MR1^{-/-}$ C57BL/6 mice, demonstrating an effector role of MAIT cells in arthritis. MAIT cells became activated upon stimulation with interleukin-23 (IL-23) or IL-1β in the absence of T cell receptor stimuli.**

Conclusion. **These results indicate that MAIT cells exacerbate arthritis by enhancing the inflammation.**

Rheumatoid arthritis (RA) is an autoimmune disease characterized by chronic inflammation in the joints. It has been suggested that environmental factors influence autoimmunity, and in particular, increasing evidence highlights the important role of gut flora in the development of autoimmune diseases (1), including arthritis. For example, differences in the intestinal microbiota of patients with early RA have been described, and tetracycline treatment was shown to reduce disease activity in RA (2,3). In addition, oral vancomycin treatment significantly decreased the severity of adjuvant-induced arthritis (4). More recently, it was demonstrated that germ-free conditions strongly inhibit arthritis in the K/BxN arthritis model and that the introduction of segmented filamentous bacteria induced severe arthritis in germ-free K/BxN mice (5). Thus, mucosal immunity plays an important role in the development and progression of arthritis.

Natural killer (NK) cells, invariant NK T (iNKT) cells, γ/δ T cells, mucosal-associated invariant T (MAIT) cells, B-1 B cells, and marginal-zone B cells are categorized as innate-like lymphocytes. Such lymphocytes reside in unique locations, including the marginal zone of the spleen and epithelial and mucosal tissues and rapidly exert effector functions in the absence of clonal expansion (6–15). Therefore, these innate-like lymphocytes are thought to play important roles in "first-line" im-

Supported by the Japan Foundation for Neuroscience and Mental Health (to Dr. Chiba), the Japan Rheumatism Foundation (to Dr. Chiba), the Japan Society for the Promotion of Science (Grants-in-Aid for Scientific Research B: 20390284 and 23390261 to Dr. Miyake), and the Ministry of Health, Labor, and Welfare of Japan (Health and Labor Sciences Research Grants on Intractable Diseases).

Asako Chiba, MD, PhD, Ryohsuke Tajima, MS, Chiharu Tomi, Yusei Miyazaki MD, PhD, Takashi Yamamura MD, PhD, Sachiko Miyake MD, PhD: National Institute of Neuroscience, National Centre of Neurology and Psychiatry, Tokyo, Japan.

Address correspondence to Sachiko Miyake MD, PhD, Department of Immunology, National Institute of Neuroscience, National Centre of Neurology and Psychiatry, 4-1-1 Ogawahigashi, Kodaira, Tokyo 187-8502, Japan. E-mail: miyake@ncnp.go.jp.

Submitted for publication May 15, 2011; accepted in revised form August 25, 2011.

mune responses against exogenous stimuli. As MAIT cells are preferentially located in the gut lamina propria, there is a growing interest in the function of MAIT cells in various types of immune responses, including autoimmunity (16–20).

MAIT cells are restricted by a nonpolymorphic class IB major histocompatibility complex (MHC) molecule, the class I MHC–related molecule (MR1), and express an invariant T cell receptor (TCR) α-chain: $V_\alpha 7.2$–$J_\alpha 33$ in humans and $V_\alpha 19$–$J_\alpha 33$ in mice. The invariant TCRα chain associates with a limited set of V_β chains (14,21,22). MAIT cells are selected in the thymus in an MR1-dependent manner, but, interestingly, MAIT cells require B cells as well as commensal flora for their peripheral expansion (14,23). Our group previously demonstrated a protective role of MAIT cells against autoimmune encephalomyelitis (EAE), an animal model of human multiple sclerosis. The suppression of EAE was accompanied by increased production of interleukin-10 (IL-10) by B cells, which was induced in part by ICOS costimulation (17). Because the invariant $V_\alpha 7.2$–$J_\alpha 33$ TCR is highly expressed in central nervous system lesions of multiple sclerosis patients, human MAIT cells may also be involved in the pathogenesis of multiple sclerosis (16).

In addition to their regulatory function, MAIT cells also possess proinflammatory functions like other innate-like lymphocytes. Le Bourhis et al (20) demonstrated that MAIT cells display antimicrobial capacity. Both human and mouse MAIT cells are activated by *Escherichia coli*–infected antigen-presenting cells in an MR1-dependent manner. MAIT cells show a protective role against *Mycobacterium abscessus* or *E coli* infections in mice. Human MAIT cells are capable of producing interferon-γ (IFNγ) and IL-17 and are found in *Mycobacterium tuberculosis*–infected lung tissues. Thus, MAIT cells play an antimicrobial function under these infectious conditions. Although accumulating evidence suggests that certain subsets of innate-like lymphocytes, such as NK cells, iNKT cells, and γ/δ T cells, are involved in the pathogenesis of arthritis in animal models of the disease, the role of MAIT cells in arthritis remains unknown (24–31).

We report herein that MAIT cells play a pathogenic role in murine models of arthritis. The disease severity of collagen-induced arthritis (CIA) in MAIT cell–deficient $MR1^{-/-}$ DBA/1J mice was ameliorated compared with that of $MR1^{+/+}$ DBA/1J mice. However, T cell responses to type II collagen (CII) and CII-specific serum antibody levels were comparable between CIA-induced $MR1^{-/-}$ and $MR1^{+/+}$ DBA/1J mice. We found that $MR1^{-/-}$ C57BL/6J mice are much less susceptible to collagen antibody–induced arthritis (CAIA) as compared to $MR1^{+/+}$ C57BL/6J mice. $MR1^{-/-}$ C57BL/6J mice reconstituted with adoptively transferred MAIT cells developed severe arthritis, suggesting that MAIT cells may be one of the effectors contributing to inflammation in arthritis. Finally, we investigated the cytokine-producing capacity of MAIT cells. No differences in IFNγ production by liver mononuclear cells (LMNCs) from $MR1^{-/-}$ C57BL/6J and $MR1^{+/+}$ C57BL/6J mice were observed upon TCR stimulation, but the level of IL-17 produced by LMNCs from $MR1^{+/+}$ C57BL/6J mice was much higher than that produced by cells from $MR1^{-/-}$ C57BL/6J mice. We further demonstrated that sorted murine MAIT cells produce IL-17 upon TCR engagement. Surprisingly, IL-17 production by MAIT cells was observed after exposure to IL-23 without TCR stimulation, and IL-1β alone induced proliferation of MAIT cells, indicating that MAIT cells may be activated by cytokines and may enhance the inflammation in arthritis.

MATERIALS AND METHODS

Mice. DBA/1J mice were purchased from the Oriental Yeast Company. C57BL/6J mice were obtained from CLEA Laboratory Animal Corporation. $MR1^{-/-}$ mice (14) were provided by S. Gilfillan (Department of Pathology and Immunology, Washington University School of Medicine, St. Louis, MO), and $V_\alpha 19$i-transgenic mice (32) on a C57BL/6J background were provided by M. Shimamura (University of Tsukuba, Ibaraki, Japan). $MR1^{-/-}$ mice were backcrossed to DBA/1J mice for 10 generations to obtain $MR1^{-/-}$ DBA/1J mice. $V_\alpha 19$i-transgenic $CD1d1^{-/-}$ C57BL/6J mice were generated by backcrossing $V_\alpha 19$i-transgenic mice with $CD1d1^{-/-}$ C57BL/6J mice for 7 generations. Mice were maintained under specific pathogen–free conditions in accordance with institutional guidelines and used in the experiments at 7–12 weeks of age.

Induction of CIA. Both $MR1^{-/-}$ DBA/1J mice and their littermate controls ($MR1^{+/+}$ DBA/1J mice) (n = 5–6 per group; ages 7–8 weeks old) were immunized intradermally at the base of the tail with 150 μg of CII (Collagen Research Center) emulsified with an equal volume of complete Freund's adjuvant containing 250 μg of heat-killed *Mycobacterium tuberculosis* H37Ra (Difco). Three weeks after the primary immunization, mice were given an intradermal booster injection of 150 μg of CII emulsified in incomplete Freund's adjuvant (Difco).

Induction of CAIA. $MR1^{-/-}$ C57BL/6J mice and their littermate controls ($MR1^{+/+}$ C57BL/6J mice) were injected intravenously with a mixture of anti-CII monoclonal antibodies (mAb) (Arthrogen-CIA mAb, 2 mg; Chondrex) followed 2 days later by an intraperitoneal injection of 50 μg of lipopolysaccharide.

Clinical assessment of arthritis. Mice were examined for signs of joint inflammation, which was scored on a scale of 0–4, where 0 = no change, 1 = significant swelling and redness

of 1 digit, 2 = mild swelling and erythema of the limb or swelling of ≥2 digits, 3 = marked swelling and erythema of the limb, and 4 = maximal swelling and redness of the limb and later, ankylosis. The average macroscopic score was expressed as a cumulative value for all paws, with a maximum possible score of 16.

Histopathologic assessment. Arthritic mice were killed, and all 4 paws were fixed in buffered formalin, decalcified, embedded in paraffin, sectioned, and then stained with hematoxylin and eosin. Histologic assessment of joint inflammation was scored on a scale of 0–3 as follows: 0 = normal joint, 1 = mild arthritis (minimal synovitis without cartilage/bone erosion), 2 = moderate arthritis (synovitis and erosion but joint architecture maintained), and 3 = severe arthritis (synovitis, erosion, and loss of joint integrity). The average of the macroscopic scores was expressed as a cumulative value for all paws, with a maximum possible score of 12.

CII-specific T cell response. Lymph node cells were collected on days 35–42 after immunization and suspended in complete RPMI 1640 medium (Life Technologies) containing 1% syngeneic mouse serum. The cells were cultured for 72 hours in 96-well flat-bottomed plates at a density of 1×10^6/well in the presence of CII. Proliferative responses were measured using a β-1205 counter (Pharmacia) to detect the incorporation of ^{3}H-thymidine (1 μCi/well) during the final 16 hours of culture.

Measurement of CII-specific total IgG, IgG1, and IgG2a. Bovine CII (1 mg/ml) was coated onto enzyme-linked immunosorbent assay (ELISA) plates (Sumitomo Bakelite) overnight at 4°C. After blocking with 1% bovine serum albumin in PBS, serially diluted serum samples were added to CII-coated wells. For detection of anti-CII antibodies, the plates were incubated with biotin-labeled anti-IgG1 and anti-IgG2a (SouthernBiotech) or anti-IgG antibody (CN/Cappel) for 1 hour and were then incubated with streptavidin–peroxidase. After adding substrate, the reaction was evaluated as the optical density values at 450 nm (OD_{450}).

Adoptive transfer and in vitro stimulation of V_α19i T cells. LMNCs were purified from V_α19i-transgenic CD1d1$^{-/-}$ C57BL/6J mice by use of Percoll density-gradient centrifugation, and erythrocytes and B cells were depleted with phycoerythrin (PE)–conjugated anti–Ter-119 and PE-conjugated anti-CD19 (BD) followed by separation with anti–PE-conjugated magnetic-activated cell sorter beads (Miltenyi Biotec). Cells were stained with fluorescein isothiocyanate–conjugated anti-TCRβ and PerCP–Cy5.5 anti-NK1.1 (BD), and TCRβ+ NK1.1+ cells were sorted using a FACSAria cell sorter (BD). The purity of isolated NK1.1+ T cells (MAIT cells) was >95%, as assessed by flow cytometry.

In adoptive transfer experiments, 5×10^5 MAIT cells or NK1.1– T cells (T cells) were injected intravenously into naive MR1$^{-/-}$ C57BL/6 recipient mice 1 day before administration of CII mAb. LMNCs or sorted MAIT cells were resuspended in RPMI 1640 medium supplemented with 10% fetal bovine serum, 2 m*M* L-glutamine, 50 units/ml of penicillin/streptomycin, and 55 μM β-mercaptoethanol (Life Technologies) and stimulated with immobilized anti-CD3 mAb (2C11, 1 μg/ml) and/or the following cytokines: IL-1β, tumor necrosis factor α (TNFα), IL-6, and transforming growth factor β (TGFβ) (all from PeproTech) and IL-23 (R&D Systems).

Detection of cytokines. Cytokine levels in the culture supernatant were determined using a sandwich ELISA. The ELISA antibodies for IFNγ were purchased from BD. Levels of IL-17 were determined using an IL-17 ELISA kit (R&D Systems).

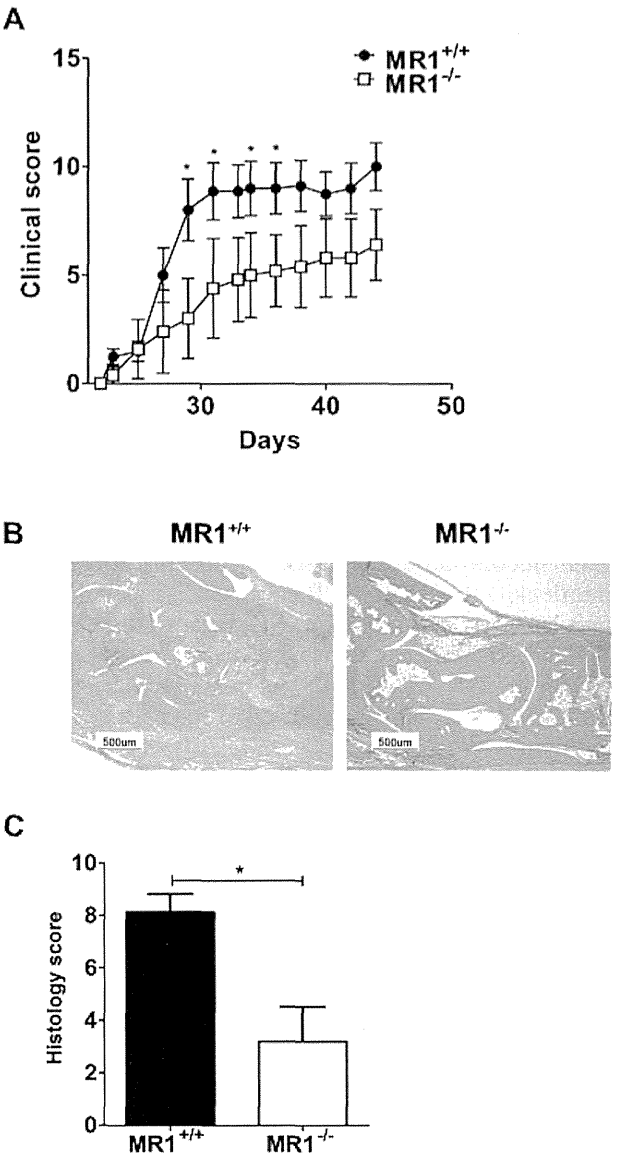

Figure 1. Amelioration of collagen-induced arthritis (CIA) in MR1$^{-/-}$ mice. **A,** Clinical scores for CIA in MR1$^{-/-}$ DBA/1J mice and in MR1$^{+/+}$ DBA/1J mice. Values are the mean ± SEM of 5–8 mice per group. * = $P < 0.05$ versus MR1$^{-/-}$ DBA/1J mice. **B,** Representative histologic sections of the joints of MR1$^{+/+}$ DBA/1J mice and MR1$^{-/-}$ DBA/1J mice. Hematoxylin and eosin stained; original magnification × 40. **C,** Histology scores in MR1$^{-/-}$ DBA/1J mice and in MR1$^{+/+}$ DBA/1J mice, expressed as the sum of the scores in the 4 paws. Results from a single representative experiment of 2 similar experiments performed are shown. Values are the mean ± SEM. * = $P < 0.05$.

Statistical analysis. Clinical or pathologic scores for CIA and CAIA in the various groups of mice are presented as